

HEAT TRANSFER IN ANNULAR PASSAGES. HYDRODYNAMICALLY DEVELOPED LAMINAR FLOW WITH ARBITRARILY PRESCRIBED WALL TEMPERATURES OR HEAT FLUXES

R. E. LUNDBERG,[†] P. A. MCCUEN[‡] and W. C. REYNOLDS[§]

(Received 19 August 1962 and in revised form 12 December 1962)

Abstract—A complete analysis for the thermal problem in hydrodynamically fully developed flow is presented. This includes evaluation of the four fundamental solutions in the thermal energy regions by solution of the eigenvalue problem, including development of asymptotic expressions for the higher eigenvalues. The analytical predictions are substantiated by their excellent agreement with careful experimental measurements reported herein. This paper is the second in a series [1] culminating a four year study of heat transfer in annular passages.¶

NOMENCLATURE

<i>a</i> ,	constant in the similarity solutions,	<i>Nu</i> ,	Nusselt number, $Nu = hD_h/k$;
	$a = E_i/3$ or $E_o/3$;	<i>Pr</i> ,	Prandtl number, $Pr = c_p\mu/k$;
<i>B</i> ,	$B = (r^{*2} - 1)/\ln r^*$;	<i>p</i> ,	similarity parameter,
<i>C_n</i> ,	constants in the eigenvalue problem;		$p = (\bar{r} - r^*)/\bar{x}^{1/3}$, or
$\hat{C}_{jj}^{(k)}$,	constants in the Leveque solutions;	<i>q</i> ,	$p = (1 - \bar{r}/\bar{x}^{1/3})$;
<i>c_p</i> ,	specific heat at constant pressure;	<i>q''</i> ,	heat rate Btu/h;
<i>D_h</i> ,	hydraulic diameter,	<i>Re</i> ,	heat flux Btu/h ft ² ;
	$D_h = 2(r_o - r_i)$;	<i>R_n(r̄)</i> ,	Reynolds number,
<i>E_i</i> ,	$E_i = N[(B/r^*) - 2r^*]$;	<i>r</i> ,	$Re = U_m \rho D_h / \mu$;
<i>E_o</i> ,	$E_o = N(2 - B)$;	\bar{r} ,	eigenfunction;
<i>f(p)</i> ,	functions in the similarity solutions;	r^* ,	radius, radial co-ordinate;
<i>G, H</i> ,	arbitrary constants;	<i>T</i> ,	$\bar{r} = r/r_o$;
$g(\bar{r})$,	function in the WKBJ solutions;	<i>t</i> ,	$r^* = r_i/r_o$;
<i>h</i> ,	convection conductance;	<i>U</i> ,	absolute temperature, °R;
<i>k</i> ,	thermal conductivity;	\bar{U} ,	temperature, °F;
<i>M</i> ,	$M = 1 + r^{*2} - B$;	<i>w(r̄)</i> ,	velocity;
<i>N</i> ,	$N = 1/2M(1 - r^*)^2$;	<i>x</i> ,	$\bar{U} = U/U_m$;
<i>n</i> ,	normal distance into fluid from the wall;	x_o ,	weight function in the Sturm-Liouville system,
			$w(\bar{r}) = N(\bar{r} - \bar{r}^3 + B\bar{r} \ln \bar{r})$;
			axial co-ordinate;
			axial co-ordinate at the step change in boundary conditions ($x_o = 0$ in the fundamental solutions);
		\bar{x} ,	$\bar{x} = (x/D_h)/(Re Pr)$.

[†] Research Engineer, Stanford Research Institute, Menlo Park, California.

[‡] Staff Scientist, Vidya, Inc., Palo Alto, California.

[§] Associate Professor, Stanford University, Stanford, California.

¶ The support of the National Aeronautics and Space Administration is gratefully acknowledged.

Greek symbols

α ,	thermal diffusivity, $= k/\rho c_p$;
γ ,	$\gamma = \int_{r^*}^1 \sqrt{[N(1 - \bar{r}^2) + B \ln \bar{r}]} d\bar{r}$;

ζ ,	$\zeta = \lambda_n^{2/3} (1 - \bar{r})$ in the WKBJ solutions;
η ,	$\eta = \lambda_n^{2/3} (\bar{r} - r^*)$;
$\theta_j^{(k)}$, $\bar{\theta}_{jj}^{(k)}$,	non-dimensional temperature;
$\theta_{ij}^{(k)}$, $\bar{\theta}_{ij}^{(k)}$,	non-dimensional wall temperatures in the fundamental solutions;
$\theta_m^{(k)}$,	non-dimensional mean temperatures;
λ ,	constant in the differential equation;
λ_n ,	eigenvalue;
μ ,	absolute viscosity;
ξ ,	axial co-ordinate in the superposition problems;
ξ_n ,	value of the axial co-ordinate at which the n th discontinuity in wall boundary conditions occurs;
ρ ,	mass density;
σ ,	dummy variable;
τ ,	shearing stress;
$\Phi_{jj}^{(k)}$, $\bar{\Phi}_{jj}^{(k)}$,	non-dimensional heat fluxes in the fundamental solutions;
ϕ ,	phase shift in the WKBJ solutions.
Subscripts	
fd ,	fully developed;
i ,	inner wall;
k ,	iteration index;
m ,	mixed mean;
n, m ,	eigenvalue and summation indices;
o ,	outer wall;
$0, 1, 2, \dots$,	defined where used.
Superscripts	
(k) ,	refers to the fundamental solution of the k th kind;
$'$,	denotes differentiation with respect to the independent variable.

INTRODUCTION

IF THE flow of a fluid in a concentric annulus is hydrodynamically fully established and the fluid has constant properties, all heat-transfer problems where the wall boundary conditions are axially symmetric can be composed from four special or fundamental boundary conditions as discussed in [1].

The fundamental solutions satisfying these boundary conditions will be solutions of the

equation for the temperature field. If the flow is laminar and the effects of viscous generation of energy and axial conduction of heat are neglected, this equation becomes

$$\frac{\partial^2 \theta}{\partial \bar{r}^2} + \frac{1}{\bar{r}} \frac{\partial \theta}{\partial \bar{r}} = \frac{U(\bar{r}) \epsilon \theta}{a - \bar{r} \bar{x}} \quad (1)$$

where

$$U(\bar{r}) = \frac{2U_m}{M} (1 - \bar{r}^2 + B \ln \bar{r}). \quad (2)$$

Laminar flow heat transfer for the cases which represent the limiting forms of the annulus (i.e. the circular tube and the parallel plane channel) has received considerable attention. Heat transfer to a fluid in laminar flow in a circular tube with constant wall temperature is the classical Graetz [2] problem. The original work by Graetz and the extension of it by Sellars, Tribus and Klein [3] comprise a relatively complete solution corresponding to the limiting geometry for the fundamental solution of the third kind. Sellars *et al.* also work out the case where the heat flux at the wall is constant by an inversion method. A direct solution for the fundamental solution of the second kind was obtained by Siegel, Sparrow and Hallman [4]. The fundamental cases, one and four, have no counterpart for flow in a circular tube.

For laminar flow in a parallel plane channel, all of the fundamental cases have significance although they are symmetric (i.e. $\theta_{ij}^{(k)} = \theta_{mj}^{(k)}$). The complete solutions of all four kinds, in a form consistent with that developed in [1] are presented by McCuen [5].

Until recently the true annulus problem has received much less attention. Jakob and Rees [6] obtained the temperature distribution valid as x tends to infinity for the fundamental solution of the second kind. Murakawa [7], [8] has presented an integral equation formulation for the solution of the first kind and a series solution approach to the same problem including the more difficult case where arbitrary peripheral variations are allowed, but he does not present numerical results. Recently Viskanta [9] has presented complete thermal entry length solu-

tions of the first and third kinds obtained with an analog computer.[†]

This problem is considered in greater length in [10] and [5], and the reader is referred there for additional detail and tabulation.

SOLUTION OF THE EQUATION

The four fundamental boundary conditions given in [1] can be made homogeneous by subtraction of the fully developed solutions, i.e. the solutions valid as \bar{x} tends to infinity. If we let[‡]

$$\tilde{\theta}_j^{(k)} = \theta_j^{(k)} - \theta_j^{(k)}/f_d \quad (3)$$

where $\theta_j^{(k)}/f_d$ is a solution to equation (1) as $\bar{x} \rightarrow \infty$, the reduced solutions, $\tilde{\theta}_j^{(k)}$, will satisfy the following boundary conditions.

1. The first kind

$$\left. \begin{aligned} \tilde{\theta}_i^{(1)}(1, \bar{x}) &= 0 \\ \tilde{\theta}_i^{(1)}(r, 0) &= -\frac{\ln \bar{r}}{\ln r^*} \end{aligned} \right\} \quad (4)$$

$$\left. \begin{aligned} \tilde{\theta}_i^{(1)}(r^*, \bar{x}) &= 0 \\ \tilde{\theta}_i^{(1)}(1, \bar{x}) &= 0 \\ \tilde{\theta}_i^{(1)}(r, 0) &= \frac{\ln \bar{r}}{\ln r^*} - 1 \\ \tilde{\theta}_i^{(1)}(r^*, \bar{x}) &= 0. \end{aligned} \right\} \quad (5)$$

2. The second kind

$$\left. \begin{aligned} \frac{\partial \tilde{\theta}_i^{(2)}}{\partial \bar{r}} &= 0, \text{ at } \bar{r} = r^* \text{ and } 1, \text{ for all } \bar{x}, \text{ and} \\ \tilde{\theta}_i^{(2)}(\bar{r}, 0) &= -\frac{r^*}{(1 + r^*)} \\ &\times \frac{1}{M(1 - r^*)^2} \left[\frac{(1 - B)}{2} (\bar{r}^2 - \ln \bar{r}) \right. \\ &- \frac{\bar{r}^4}{8} + \frac{B}{2} \bar{r}^2 \ln \bar{r} - \frac{(r^*)^2 M}{2} \\ &\left. + \frac{(1 + \ln r^*)}{2} + \frac{(r^*)^4}{8} \right] \\ &- [\theta_{ii}^{(2)} - \theta_{mo}^{(2)}] f_d. \end{aligned} \right\} \quad (6)$$

[†] After this paper had been prepared, the work of Hatton and Quarmby [16] appeared in the *International Journal of Heat and Mass Transfer*. They have considered the solutions of the second and the third kinds when heating occurs at the inner wall only.

[‡] The notation used here is described in [1].

$$\left. \begin{aligned} \frac{\partial \tilde{\theta}_o^{(2)}}{\partial \bar{r}} &= 0 \text{ at } \bar{r} = r^* \text{ and } 1, \text{ for all } \bar{x} \text{ and} \\ \tilde{\theta}_o^{(2)}(\bar{r}, 0) &= \frac{1}{(1 + r^*) M(1 - r^*)} \\ &\times \frac{(1 - B)}{2} (\bar{r}^2 - 1) - \frac{(\bar{r}^4 - 1)}{8} \\ &+ \frac{B}{2} \bar{r}^2 \ln \bar{r} - \frac{(r^*)^2}{2} [(r^*)^2 - B] \ln \bar{r} \\ &- [\theta_{oo}^{(2)} - \theta_{mo}^{(2)}] f_d. \end{aligned} \right\} \quad (7)$$

3. The third kind

$$\left. \begin{aligned} \theta_i^{(3)}(r^*, \bar{x}) &= 0; \\ \bar{\Phi}_i^{(3)}(1, \bar{x}) &= 0 \text{ and } \tilde{\theta}_i^{(3)}(\bar{r}, 0) = -1, \\ \tilde{\theta}_o^{(3)}(1, \bar{x}) &= 0, \end{aligned} \right\} \quad (8)$$

$$\bar{\Phi}_o^{(3)}(r^*, \bar{x}) = 0 \text{ and } \tilde{\theta}_o^{(3)}(\bar{r}, 0) = -1. \quad (9)$$

4. The fourth kind

$$\left. \begin{aligned} \bar{\Phi}_i^{(4)}(r^*, \bar{x}) &= 0, \\ \tilde{\theta}_i^{(4)}(1, \bar{x}) &= 0, \\ \tilde{\theta}_i^{(4)}(\bar{r}, 0) &= \frac{r^*}{2(1 - r^*)} \ln \bar{r}, \\ \tilde{\Phi}_o^{(4)}(1, \bar{x}) &= 0, \\ \tilde{\theta}_o^{(4)}(r^*, \bar{x}) &= 0 \end{aligned} \right\} \quad (10)$$

and

$$\tilde{\theta}_o^{(4)}(\bar{r}, 0) = -\frac{1}{2(1 - r^*)} \ln \left(\frac{\bar{r}}{r^*} \right). \quad (11)$$

For small values of the axial co-ordinate \bar{x} the energy equation can be reduced by neglecting the curvature of the velocity profile and approximating it by a linear equation using the wall slope of the actual velocity. This is the Leveque [11] approximation and is justified by the fact that very near the step change in boundary conditions the temperature signal has penetrated only a short distance into the fluid.

The reduced equations are

$$\frac{\partial^2 \theta}{\partial \bar{r}^2} = E_i (\bar{r} - r^*) \frac{\partial \theta}{\partial \bar{x}} \quad (12)$$

and

$$\frac{\partial^2 \theta}{\partial \bar{r}^2} = E_o (\bar{r} - 1) \frac{\partial \theta}{\partial \bar{x}} \quad (13)$$

when the non-zero boundary condition is applied to the inner and the outer walls respectively.

For the fundamental solutions of the first and third kinds, equations (12) and (13) can be solved by seeking similarity solutions of the form $\theta = f(p)$ where $p = (\bar{r} - r^*)/\bar{x}^{1/3}$ or $p = (\bar{r} - 1)/\bar{x}^{1/3}$. From these solutions one can obtain

$$\Phi_{ii}^{(k)} = 2.2396 (1 - r^*)$$

$$\left[\frac{(B/r^*) - 2r^*}{18(1 - r^*)^2 M} \right]^{1/3} \bar{x}^{-1/3} \quad (14)$$

$$\theta_{mi}^{(k)} = \left(\frac{6r^*}{1 + r^*} \right) 2.2396 (1 - r^*)$$

$$\left[\frac{(B/r^*) - 2r^*}{18(1 - r^*)^2 M} \right]^{1/3} \bar{x}^{2/3} \quad (15)$$

$$\Phi_{oo}^{(k)} = -2.2396 (1 - r^*)$$

$$\left[\frac{B - 2}{18(1 - r^*)^2 M} \right]^{1/3} \bar{x}^{-1/3} \quad (16)$$

$$\theta_{mo}^{(k)} = -\left(\frac{6}{1 + r^*} \right) 2.2396 (1 - r^*)$$

$$\left[\frac{B - 2}{18(1 - r^*)^2 M} \right]^{1/3} \bar{x}^{2/3} \quad (17)$$

for $k = 1$ or 3 .

For the fundamental solutions of the second and fourth kinds we will set $\theta = \bar{x}^{1/3} f(p)$. Where p is as previously defined. There results

$$\theta_{ii}^{(k)} = \frac{0.36925}{(1 - r^*)} \left[\frac{(B/r^*) - 2r^*}{18(1 - r^*)^2 M} \right]^{-1/3} \bar{x}^{1/3} \quad (18)$$

$$\theta_{oo}^{(k)} = -\frac{0.36925}{(1 - r^*)} \left[\frac{B - 2}{18(1 - r^*)^2 M} \right]^{-1/3} \bar{x}^{1/3} \quad (19)$$

Table 1 summarizes the coefficients in equations (14)–(19). The symbols used are as follows

$$\Phi_{jj}^{(k)} = \hat{C}_{jj}^{(k)} \bar{x}^{-1/3},$$

$$\theta_{mj}^{(k)} = \hat{C}_{mj}^{(k)} \bar{x}^{2/3}, \text{ for } j = i \text{ or } o, k = 1 \text{ and } 3$$

and

$$\theta_{ji}^{(k)} = \hat{C}_{ij}^{(k)} \bar{x}^{1/3}, \text{ for } j = i \text{ or } o, k = 2 \text{ and } 4.$$

The complete equation (1) can be solved by separation of variables giving

$$\theta_i^{(k)} = (\theta_j^{(k)})_{fd} = \sum_{n=0}^{\infty} (C_n)_j^{(k)} R_n^{(k)} \exp(-\lambda_n^{(k)} \bar{x}) \quad (20)$$

where $R_n^{(k)}$ satisfies the Sturm–Liouville equation

$$\frac{d^2 R_n^{(k)}}{d\bar{r}^2} - \frac{1}{\bar{r}} \frac{dR_n^{(k)}}{d\bar{r}} + \lambda_n^{(k)} N(1 - \bar{r}^2 + B \ln \bar{r}) R_n^{(k)} = 0. \quad (21)$$

The λ_n , $n = 0, 1, 2, \dots$ comprise an infinite set of eigenvalues for which $R_n^{(k)}$ will satisfy the boundary conditions at $\bar{r} = r^*$ and 1 as specified for the reduced solutions of the k th kind.

The coefficients of the series in (20) are given by

$$(C_n)_j^{(k)} = \frac{\int_{r^*}^1 w(\bar{r}) \theta_{ji}^{(k)}_{fd} R_n^{(k)} d\bar{r}}{\int_{r^*}^1 w(\bar{r}) [R_n^{(k)}]^2 d\bar{r}} \quad (22)$$

where

$$w(\bar{r}) = N(\bar{r} - \bar{r}^3 + B\bar{r} \ln \bar{r}). \quad (23)$$

Equation (21) was solved directly using the iterative method of Berry and de Prima [12] together with a numerical integration procedure given by Hamming [13]. This method may be summarized as follows.

If $(\lambda_n^{(k)})_k$ is the k th approximation to the desired

Table 1. Constants in the limiting (small \bar{x}) approximations to the fundamental solutions

r^*	$\hat{C}_{ii}^{(1)} = \hat{C}_{ii}^{(3)}$	$\hat{C}_{oo}^{(1)} = \hat{C}_{oo}^{(3)}$	$\hat{C}_{mo}^{(1)} = \hat{C}_{mo}^{(3)}$	$\hat{C}_{mo}^{(1)} = \hat{C}_{mo}^{(3)}$	$\hat{C}_{ii}^{(2)} = \hat{C}_{ii}^{(4)}$	$\hat{C}_{oo}^{(4)} = \hat{C}_{oo}^{(4)}$
0	∞	1.076	0	6.460	0	0.7680
0.02	2.186	1.127	0.2572	6.630	0.3782	0.7337
0.05	1.795	1.138	0.5129	6.506	0.4605	0.7262
0.10	1.583	1.149	0.8636	6.270	0.5223	0.7193
0.20	1.427	1.164	1.427	5.822	0.5794	0.7101
0.40	1.319	1.185	2.261	5.082	0.6267	0.6973
0.60	1.274	1.203	2.867	4.511	0.6489	0.6874
0.80	1.249	1.218	3.331	4.061	0.6620	0.6786
1.0	1.233	1.233	3.700	3.700	0.6709	0.6709

value, λ_n^2 , and $[R_n(\bar{r})]_k$ is a solution to equation (21) with $\lambda^2 = (\lambda_n^2)_k$ such that $(R_n)_k$ satisfies the requisite boundary condition only at $\bar{r} = r^*$; and if

$$\int_{r^*}^1 w(\bar{r}) (R_n)_k^2 d\bar{r} = 1 \quad (24)$$

then the next approximation is given by

$$(\lambda^2)_{k+1} = (\lambda_n^2)_k \pm [R_n(1)]_k [R'_n(1)]_k. \quad (25)$$

This sequence of approximations converges monotonically to λ_n^2 . In (25) the plus (+) sign is associated with the condition of zero derivative desired at the outer wall ($\bar{r} = 1$), and the minus (-) sign with zero ordinate.

A value is assumed for either the slope or the ordinate at $\bar{r} = r^*$, (whichever is not specified as zero by the boundary condition) and equation (21) integrated numerically. The outer wall values are adjusted in accordance with (24), then the value of λ_n^2 is corrected by (25) and the process is repeated.

The logarithmic term in the differential equation does not pose any fundamental difficulty with this method, in fact $w(\bar{r})$ need not be an explicit algebraic form at all, so this method can readily be applied to these same problems in turbulent flow.

The computation of these solutions has been performed on the Burroughs 220 Electronic Digital Computer at the Stanford University computation center. The nature of the computation is such that the values of the expansion coefficients are obtained directly from (22) using a simple numerical integration. The condition (24) makes the denominator of (22) always equal to unity.

The eigenvalues and the pertinent combinations† of constants are given in Tables 2-5.

† The forms of these combinations are apparent from equation (20) and the definition of $\Phi_r^{(k)}$.

Table 2. Functions in the fundamental solutions of the first kind

r^*	n	$(\lambda_n)^{(1)}$	$(\lambda_n^2)^{(1)}$	$\cdot(C_n)_i^{(1)} R_n(r^*)$	$\cdot(C_n)_i^{(1)} R_n'(r^*)$	$\cdot(C_n)_o^{(1)} R_n(r^*)$	$\cdot(C_n)_o^{(1)} R_n'(r^*)$
		$2(1 - r^*)$	$2(1 - r^*)$	$2(1 - r^*)$	$2(1 - r^*)$	$2(1 - r^*)$	$2(1 - r^*)$
0.02	0	4.748	22.54	-10.22	+0.8076	-40.25	+3.179
	1	10.87	118.2	-6.392	-0.5494	+27.37	+2.353
	2	16.99	228.8	-5.065	+0.4524	-22.55	+2.014
	3	23.10	533.8	-4.353	-0.3978	+19.82	+1.811
0.05	0	4.939	24.39	-6.697	+1.038	-20.77	+3.221
	1	11.18	125.0	-4.457	-0.7306	+14.62	+2.397
	2	17.40	303.0	-3.647	+0.6117	-12.24	+2.053
	3	23.62	538.3	-3.200	-0.5437	+10.88	+1.848
0.1	0	5.105	26.06	-5.171	+1.297	-12.97	+3.255
	1	11.43	130.7	-3.618	-0.9387	+9.389	+2.435
	2	17.75	315.3	-3.029	+0.7956	-7.958	+2.090
	3	24.07	579.4	-2.694	-0.7122	+7.124	+1.883
0.25	0	5.323	28.33	-5.056	+1.829	-7.317	+3.299
	1	11.75	138.2	-3.008	-1.370	+5.480	+2.496
	2	18.19	331.0	-2.513	+1.176	-4.703	+2.149
	3	24.63	606.6	-2.315	-1.059	+4.237	+1.938
0.5	0	5.445	29.65	-3.636	+2.465	-4.931	+3.343
	1	11.93	142.3	-2.770	-1.881	+3.762	+2.554
	2	18.43	339.6	-2.388	+1.622	-3.245	+2.204
	3	24.93	621.6	-2.156	-1.465	+2.930	+1.990
1.0	0	5.492	30.16	-3.432	+3.432	-3.432	+3.432
	1	11.99	143.8	-2.608	-2.608	+2.608	+2.608
	2	18.51	342.9	-2.277	+2.277	-2.277	+2.277
	3	25.04	627.3	-2.058	-2.058	+2.058	+2.058

Table 3. Functions in the fundamental solutions of the second kind

r^*	n	$(\lambda_n)^{(2)}$	$(\lambda_n^2)^{(2)}$	$(C_n)_r^{(2)} R_n(r^*)$	$(C_n)_r^{(2)} R_n(1)$	$(C_n)_o^{(2)} R_n(r^*)$	$(C_n)_o^{(2)} R_n(1)$
0	1	7.166	51.35	0	0	+0.2017	-0.09936
	2	12.95	167.7	0	0	-0.08755	-0.03462
	3	18.66	348.3	0	0	+0.05297	-0.01826
	4	24.35	593.0	0	0	-0.03664	-0.01150
0.01	1	7.507	56.35	-0.003473	+0.001795	+0.1795	-0.09278
	2	13.62	185.5	-0.001789	-0.007589	-0.07589	-0.03219
0.02	1	7.538	56.83	-0.006653	+0.003501	+0.1750	-0.09215
	2	13.70	187.8	-0.003341	-0.001461	-0.07305	-0.03192
	3	19.80	393.3	-0.002182	+0.0008562	+0.04280	-0.01679
	4	25.89	670.4	-0.001603	-0.0005839	-0.02901	-0.01055
0.035	1	7.557	57.11	-0.01106	+0.005958	+0.1702	-0.09171
0.05	1	7.562	57.18	-0.01511	+0.008316	+0.1663	-0.09151
	2	13.81	190.8	-0.007161	-0.003361	-0.06723	-0.03156
	3	20.01	400.5	-0.004472	+0.001924	+0.03848	-0.01656
	4	26.20	686.5	-0.003149	-0.001280	-0.02560	-0.01040
0.075	1	7.559	57.14	-0.02121	+0.01205	+0.1607	-0.09139
0.1	1	7.550	57.00	-0.02663	+0.01650	+0.1560	-0.09139
	2	13.88	192.7	-0.01172	-0.006057	-0.06058	-0.03129
	3	20.17	407.1	-0.006969	+0.003376	+0.03379	-0.01636
	4	26.46	700.5	-0.004740	-0.002205	-0.02205	-0.01026
	5	32.75	1073.0	-0.003479	+0.001574	+0.01574	-0.007122
	6	39.04	1524.0	-0.002687	-0.001191	-0.01191	-0.005278
0.175	1	7.515	56.48	-0.03975	+0.02523	+0.1441	-0.09149
0.25	1	7.484	56.01	-0.04940	+0.03364	+0.1345	-0.09145
	2	13.95	194.7	-0.01914	-0.01213	-0.04853	-0.03076
	3	20.39	415.9	-0.01061	+0.006510	+0.02604	-0.01597
	4	26.82	719.7	-0.006890	-0.004146	-0.01659	-0.009983
0.375	1	7.445	55.43	-0.06095	+0.04558	+0.1215	-0.09089
0.5	1	7.420	55.06	-0.06966	+0.05552	+0.1110	-0.08981
	2	13.98	195.6	-0.02421	-0.01899	-0.03799	-0.02980
	3	20.51	421.0	-0.01288	+0.009971	+0.01994	-0.01543
	4	27.0	731.0	-0.008178	-0.006276	-0.01255	-0.009633
0.7	1	7.399	54.75	-0.07652	+0.06841	+0.09775	-0.08739
1.0	1	7.391	54.63	-0.08301	+0.08301	+0.08301	-0.08301
	2	14.00	196.0	-0.02777	-0.02777	-0.02777	-0.02777
	3	20.56	423.0	-0.01446	+0.01446	+0.01446	-0.01446
	4	27.12	735.5	-0.008670	-0.008670	-0.008670	-0.008670

Table 4. Functions in the fundamental solutions of the third and fourth kinds

r^*	n	$(\lambda_n)_i^{(3)} = (\lambda_n)_o^{(4)}$	$(\lambda_n)^2$	$2(1 - r^*) \cdot (C_n)_i^{(3)} R_n'(r^*)$	$(C_n)_i^{(3)} R_n(1)$	$2(1 - r^*) \cdot (C_n)_o^{(4)} R_n'(r^*)$	$(C_n)_o^{(4)} R_n'(1)$
		$(\lambda_n)_i^{(3)}$	$(\lambda_n)^2$	$\cdot (C_n)_i^{(3)} R_n'(r^*)$	$(C_n)_i^{(3)} R_n(1)$	$\cdot (C_n)_o^{(4)} R_n'(r^*)$	$(C_n)_o^{(4)} R_n'(1)$
0.02	0	1.529	2.536	-31.77	-1.073	-53.50	-1.807
	1	8.455	71.50	-7.590	+0.1080	+5.363	-0.07633
	2	14.70	216.2	-5.527	-0.0563	-2.815	-0.02869
	3	20.87	435.6	-4.608	+0.0378	+1.876	-0.01541
0.05	0	1.823	3.325	-17.11	-1.092	-21.85	-1.395
	1	8.734	76.29	-5.173	+0.1369	+2.739	-0.07252
	2	15.08	227.6	-3.932	-0.0734	-1.470	-0.02747
	3	21.36	456.4	-3.361	+0.0501	+1.002	-0.01495
0.1	0	2.050	4.203	-11.21	-1.112	-11.12	-1.104
	1	8.978	80.60	-4.126	+0.1686	+1.686	-0.06894
	2	15.41	237.6	-3.239	-0.0925	-0.9249	-0.02646
	3	21.78	474.5	-2.815	+0.0638	+0.6386	-0.01448
0.25	0	2.428	5.896	-6.989	-1.152	-4.609	-0.7599
	1	9.310	86.69	-3.356	+0.2305	+0.9223	-0.06336
	2	15.84	251.0	-2.727	-0.1303	-0.5213	-0.02490
	3	22.32	498.4	-2.407	+0.0909	+0.3639	-0.01375
0.5	0	2.766	7.650	-5.302	-1.194	-2.389	-0.5385
	1	9.535	90.92	-3.045	+0.2976	+0.5953	-0.05818
	2	16.10	259.3	-2.518	-0.1717	-0.3435	-0.02343
	3	22.64	512.6	-2.236	+0.1208	+0.2416	-0.01305
1.0	0	3.117	9.721	-4.353	-1.248	-1.248	-0.3580
	1	9.714	94.36	-2.854	+0.3831	+0.3932	-0.05145
	2	16.26	264.6	-2.387	-0.2263	-0.2264	-0.02146
	3	22.81	520.3	-2.127	+0.1605	+0.1607	-0.01212

The values for the circular tube ($r^* = 0$) are from Lipkis [14] and Siegel, Sparrow, and Hallman [4].†

The computation of the higher modes of equation (21) becomes increasingly difficult due to the fact that the eigenfunctions oscillate (undergo a sign change) n times in the internal $r^* \leq \bar{r} \leq 1$. To follow these oscillations, the spacing in the finite difference net must be

† A direct comparison for $r^* = 0.5$ can be made with the values reported by Hatton and Quarmby [16]. They used an iterative digital calculation similar to the approach presented here. Because of the method used to define the dimensionless parameters, the eigenvalues reported by Hatton and Quarmby must be multiplied by a factor of two to be numerically consistent with the present results. They give (retaining four figures) $(\lambda_3)_i^{(3)} = 22.64$ and $(\lambda_4)_i^{(3)} = 27.04$. These values coincide with those in Tables 3 and 4.

reduced. The adequacy of the numerical solution is ultimately limited by the accumulation of round off and truncation errors in the integration. Further, because of the number of boundary conditions involved, the calculation by machine of many eigenvalues and functions entails considerable expense. Accordingly, we would like to develop an asymptotic solution valid as λ_n becomes large. Following the method of Sellars, Tribus and Klein [3], the so-called WKBJ solution to equation (20) can be obtained.

Let

$$R_n = e^{g(\bar{r})} \quad (26)$$

and assume a solution of the form

$$g(\bar{r}) = \lambda g_0 + g_1 + \lambda^{-1} g_2 + \dots \quad (27)$$

Since λ_n is assumed to be large, only the first

Table 5. Functions in the fundamental solutions of the third and fourth kinds

r^*	n	$(\lambda_n)_t^{(4)} = (\lambda_n)_n^{(3)}$	$(\lambda_n)^2$	$(C_n)_t^{(1)} R_n(r^*)$	$(C_n)_t^{(1)} R_n'(1)$	$(C_n)_n^{(3)} R_n(r^*)$	$(C_n)_n^{(3)} R_n'(1)$
0	0	3.824	14.62	0	0	1.466	+2.995
	1	9.445	89.21	0	0	+0.8024	+2.176
	2	15.09	227.8	0	0	-0.5870	+1.851
	3	20.74	430.4	0	0	-0.4749	+1.660
0.02	0	3.957	15.66	-0.01274	+0.02899	-1.449	+3.297
	1	9.947	98.94	-0.004716	-0.01500	+0.7504	+2.388
	2	15.97	255.3	-0.002771	+0.01061	0.5306	+2.032
	3	22.02	485.0	-0.001916	-0.008361	+0.4180	+1.824
0.05	0	3.931	15.45	-0.03051	+0.07165	-1.433	+3.364
	1	9.991	99.82	-0.01046	-0.03573	-0.7147	+2.441
	2	16.11	259.7	-0.005835	+0.02463	-0.4926	+2.079
	3	22.26	495.5	-0.003874	-0.01901	+0.3803	+1.867
0.1	0	3.867	14.95	-0.05792	+0.1410	1.410	+3.434
	1	9.994	99.88	-0.01788	-0.06684	+0.6685	+2.498
	2	16.20	262.7	-0.009377	+0.04467	0.4467	+2.128
	3	22.45	504.2	-0.005966	-0.03377	+0.3375	+1.910
0.25	0	3.680	13.54	-0.1287	+0.3400	1.360	+3.594
	1	9.936	98.74	-0.03154	-0.1433	+0.5734	+2.605
	2	16.30	265.7	-0.01491	+0.09083	0.3633	+2.213
	3	22.69	515.1	-0.008924	-0.06651	+0.2660	+1.983
0.5	0	3.436	11.81	-0.2219	+0.6535	1.307	+3.484
	1	9.845	96.93	-0.04242	-0.2400	+0.4800	+2.716
	2	16.32	266.5	-0.01865	+0.1462	0.2924	+2.291
	3	22.81	520.6	0.01078	0.1050	0.2101	+2.048
1.0	0	3.117	9.721	-0.3580	-1.248	1.248	+4.355
	1	9.714	94.36	-0.05145	-0.3932	+0.3831	+2.854
	2	16.26	264.6	-0.02146	+0.2264	-0.2263	+2.387
	3	22.81	520.3	0.01212	-0.1607	+0.1605	+2.127

two terms of (27) are retained. By substituting (26) and (27) into (20), the resulting equations for g_0 and g_1 can be solved yielding the WKBJ solution

$$R_n(\bar{r}) = \frac{G_n \cos \left\{ \lambda_n \int_{\bar{r}_*}^{\bar{r}} \sqrt{[N(1 - \bar{r}^2 + B \ln \bar{r})] d\bar{r}} - \phi \right\}}{\sqrt{(\bar{r})} [N(1 - \bar{r}^2 + B \ln \bar{r})]^{1/4}} \quad (28)$$

This solution must be patched to the regular solution of (20) near the boundary walls.

If we again assume that very near the wall the velocity profile can be expressed as a linear

equation, (20) can be reduced to two simpler equations.

Near the inner wall we have

$$\frac{d^2 R_n}{d\eta^2} + \frac{1}{\lambda_n^{2/3} (r^* + \eta/\lambda_n^{2/3})} \frac{dR_n}{d\eta} + E_i \eta R_n = 0. \quad (29)$$

If λ_n is large, (29) becomes

$$\frac{d^2 R_n}{d\eta^2} + E_i \eta R_n = 0 \quad (30)$$

which is a form of Bessel's equation. The solution to (30) is

$$R_n = G_1 \eta^{1/2} J_{1/3} \left[\frac{2\sqrt{(E_i)}}{3} \eta^{3/2} \right] \quad (\lambda_n)^{(2)} = (n + 1/6) \frac{\pi}{\gamma} \quad (41)$$

$$+ H_1 \eta^{1/2} J_{-1/3} \left[\frac{2\sqrt{(E_i)}}{3} \eta^{3/2} \right]. \quad (31) \quad (\lambda_n)^{(3)} = (\lambda_n)^{(4)} = (n + 1/2) \frac{\pi}{\gamma}. \quad (42)$$

Near the outer wall, again assuming λ to be large, (20) becomes

$$\frac{d^2 R_n}{d\zeta^2} + E_0 \zeta R_n = 0. \quad (32)$$

Which has the solution

$$R_n = G_2 \zeta^{1/2} J_{1/3} \left[\frac{2\sqrt{(E_0)}}{3} \zeta^{3/2} \right] + H_2 \zeta^{1/2} J_{-1/3} \left[\frac{2\sqrt{(E_0)}}{3} \zeta^{3/2} \right]. \quad (33)$$

The patching of equations (28)–(31) and (33) can be performed by appropriately linearizing the expression for the velocity profile in (28) and by noting that for large values of the argument the Bessel functions appearing in (31) and (33) can be expressed as cosine functions. This results in demanding that

$$G_0 = \sqrt{(r^*)} / \sqrt{\left(\frac{\pi}{3}\right)} \lambda^{1/6} \quad (34)$$

and the following equations for the constants G_1 , H_1 , G_2 and H_2 :

$$G_1 \cos(5\pi/12) + H_1 \cos(\pi/12) = \cos \phi \quad (35)$$

$$G_1 \sin(5\pi/12) + H_1 \sin(\pi/12) = \sin \phi \quad (36)$$

$$G_2 \cos(5\pi/12) + H_2 \cos(\pi/12) = r^* \cos(\gamma\lambda - \phi) \quad (37)$$

$$G_2 \sin(5\pi/12) + H_2 \sin(\pi/12) = r^* \sin(\gamma\lambda - \phi) \quad (38)$$

where

$$\gamma = \int_{r^*}^1 \sqrt{N(1 - \tilde{r}^2 + B \ln \tilde{r})} d\tilde{r}. \quad (39)$$

To evaluate ϕ , and hence equations (35)–(38), the appropriate boundary conditions for each of the fundamental cases must be applied.

The asymptotic forms of the eigenvalues, λ_n , are given by the following expressions:

$$(\lambda_n)^{(1)} = (n + 5/6) \frac{\pi}{\gamma} \quad (40)$$

Values of γ and π/γ are given in Table 6.

Table 6. Constants in the asymptotic (large λ) solutions

r^*	γ	π/γ
0.0	0.5553	5.656
0.01	0.5221	6.016
0.02	0.5162	6.085
0.03	0.5122	6.132
0.04	0.5091	6.169
0.05	0.5067	6.199
0.06	0.5046	6.225
0.07	0.5028	6.247
0.08	0.5012	6.267
0.09	0.4998	6.284
0.10	0.4986	6.300
0.20	0.4907	6.401
0.30	0.4867	6.454
0.40	0.4843	6.485
0.50	0.4829	6.505
0.60	0.4820	6.517
0.70	0.4814	6.525
0.80	0.4811	6.529
1.00	0.4809	6.531

The expansion coefficients, C_n , can be expressed in terms of the wall values of R_n and the derivatives of R_n with respect to \tilde{r} and λ .

The asymptotic forms of the relevant combinations of the expansion coefficients and the ordinates or derivatives at the boundary walls can be constructed using the appropriate equations for R_n . This construction is presented in detail in [10].

The values given in Tables 2–5 permit a determination of the adequacy of the asymptotic expressions for the eigenvalues and the eigenconstants. Equations (40)–(42) provide an estimate of the eigenvalues which is within 1 per cent for all $n \geq 4$. The expressions for the constants, however, provide some difficulty when the radius ratio is small, particularly those evaluated at the inner wall or where the non-zero boundary condition is applied at the inner wall. The origin of this difficulty can be seen from an

inspection of equation (29). If r^* is small, (note that η is also small), λ_n must be very large to make equation (30) a reasonable approximation. For $r^* = 0.1$, λ_4 is not sufficiently large to permit this approximation.

The asymptotic expressions for the series constants have a consistent form such that the absolute values of the terms can be expressed as a constant factor (which is a function of radius ratio, r^*) multiplied by a power of the eigenvalue, λ_n . For example

$$2(1 - r^*) (C_n)^{(1)} [\partial R_n^{(1)} / \partial r]_{r=r^*} \sim K(r^*) \lambda_n^{-s} \quad (43)$$

where, for the various forms, $K(r^*)$ and S depend on the wall boundary conditions. Some of the series constants alternate in sign and the appropriate algebraic signs of any terms can readily be deduced from an inspection of the tabulated values.

Because of the difficulty previously noted, the form of the asymptotic expressions is used to provide an estimate of the next succeeding eigenconstants beyond those given in Tables 2-5. Fig. 1 is a logarithmic plot of the absolute value of the quantity $2(1 - r^*) (C_n)^{(1)} [\partial R_n^{(1)} / \partial r]_{r=r^*}$ as a function of λ_n , for $r^* = 0.02$. Since the constants for $n = 1, 2$, and 3 lie on a nearly straight line, an extrapolation line is constructed to pass through the last two. The values of the constants are taken as the ordinates on this line at the values of λ_n given by the asymptotic expression. Notice that an equation for the values obtained in this manner will also have the form $K(r^*) \lambda_n^{-s}$ although the values of $K(r^*)$ and S

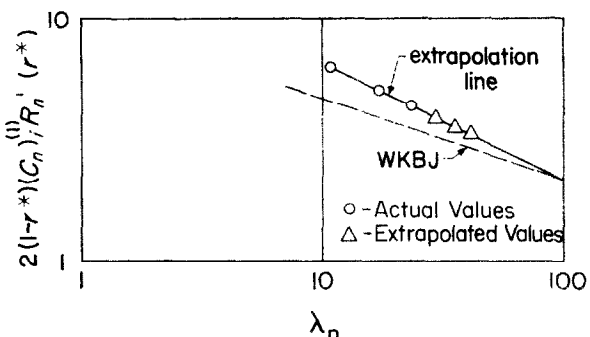


FIG. 1. Estimation of higher eigen-constants for small radius ratios.

will, in general, differ from those resulting from the asymptotic expressions.

The values of $K(r^*)$ and S obtained from the graphical extrapolation scheme together with the coefficients derived from the WKBJ solutions are given in Tables 7-10. For any given combination of constants the exponent, S , in the WKBJ forms is independent of r^* and is given at the bottom of the pertinent column in the tables.

For $r^* = 0.5$, the eigen-constants predicted by the WKBJ expression are within 5 per cent for $n \geq 4$. For the cases where the non-zero boundary condition is at the outer wall and the expansion constants involve the ordinates or derivatives of the eigenfunctions at the outer wall, the WKBJ method gives good results even for small r^* . For all other cases, however, the graphical extrapolation method should be used. Eventually (i.e. for λ_n sufficiently large) the WKBJ solution should become valid, and it is

Table 7. Asymptotic values of the functions in the fundamental solutions of the first kind

r^*	$2(1 - r^*) (C_n)_0 R_n'(r^*)$			$2(1 - r^*) (C_n)_1 R_n'(1)$			$2(1 - r^*) (C_n)_n R_n'(r^*)$			$2(1 - r^*) (C_n)_n R_n'(1)$		
	K WKBJ	K Graph	S	K WKBJ	K Graph	S	K WKBJ	K Graph	S	K WKBJ	K Graph	S
0	∞			0			∞			4.547		
0.02	9.930	20.2	0.490	1.008	1.515	0.427	50.42	73.1	0.420	5.121	5.40	0.348
0.05	8.321	11.62	0.408	1.481	1.805	0.378	29.61	37.8	0.396	5.270	5.43	0.340
0.1	7.448	9.17	0.392	2.007	2.08	0.335	20.07	22.9	0.368	5.409	5.44	0.334
0.2	6.821			2.756			13.78			5.566		
0.25	6.662	6.77	0.336	3.059	3.07	0.334	12.23	12.9	0.347	5.620	5.63	0.334
0.3	6.549			3.337			11.12			5.668		
0.4	6.389			3.830			9.576			5.742		
0.5	6.281	6.28	0.334	4.269	4.29	0.334	8.538	8.58	0.334	5.802	5.85	0.334
0.6	6.201			4.667			7.779			5.854		
0.7	6.139			5.035			7.193			5.899		
0.8	6.090			5.380			6.725			5.940		
1.0	6.036			6.036			6.036			6.036		
S	1/3			1/3			1/3			1/3		

Table 8. Asymptotic values of the functions in the fundamental solutions of the second kind

r^*	$(C_n)_i R_n(r^*)$			$(C_n)_i R_n(1)$			$(C_n)_o R_n(r^*)$			$(C_n)_o R_n(1)$		
	K WKBJ	K Graph	S	K WKBJ	K Graph	S	K WKBJ	K Graph	S	K WKBJ	K Graph	S
0	0		0				∞			2.138		
0.02	1.133	0.0714	1.162	0.2232	0.0677	1.462	11.16	3.020	1.423	2.138	2.78	1.71
0.05	1.403	0.2065	1.280	0.3944	0.198	1.54	7.889	3.86	1.535	2.216	2.72	1.70
0.1	1.619	0.533	1.442	0.6011	0.394	1.582	6.011	3.94	1.582	2.230	2.54	1.68
0.2	1.826			0.9040			4.520			2.237		
0.25	1.886	1.122	1.542	1.027	0.863	1.622	4.108	4.00	1.66	2.236	2.51	1.68
0.3	1.933			1.138			3.794			2.234		
0.4	2.001			1.335			3.337			2.226		
0.5	2.047	1.78	1.625	1.506	1.46	1.645	3.013	3.13	1.66	2.216	2.45	1.68
0.6	2.081			1.659			2.766			2.205		
0.7	2.108			1.799			2.570			2.193		
0.8	2.128			1.927			2.408			2.181		
1.0	2.148			2.148			2.148			2.148		
S	5/3		5/3				5/3			5/3		

Table 9. Asymptotic values of the functions in the fundamental solutions of the third kind

r^*	$2(1 - r^*) (C_n)_i R_n'(r^*)$			$(C_n)_i R_n(1)$			$(C_n)_o R_n(r^*)$			$2(1 - r^*) (C_n)_o R_n'(1)$		
	K WKBJ	K Graph	S	K WKBJ	K Graph	S	K WKBJ	K Graph	S	K WKBJ	K Graph	S
0	∞		0				∞			4.547		
0.02	9.930	12.40	0.520	0.6607	1.21	1.142	17.03	4.38	0.758	5.121	5.09	0.329
0.05	8.321	12.12	0.428	0.9603	1.480	1.105	12.16	4.72	0.813	5.270	5.26	0.333
0.10	7.448	9.84	0.406	1.289	1.773	1.080	9.360	4.91	0.859	5.409		
0.20	6.821			1.747			7.129			5.566		
0.25	6.662	7.13	0.350	1.929	2.190	1.021	6.512	5.33	0.960	5.620		
0.3	6.549			2.095			6.044			5.668		
0.4	6.389			2.385			5.359			5.742		
0.5	6.281	6.37	0.338	2.638	2.86	1.012	4.875	4.60	0.983	5.802		
0.6	6.201			2.864			4.507			5.854		
0.7	6.139			3.070			4.215			5.899		
0.8	6.090			3.260			3.975			5.940		
1.0	6.036			3.601			3.601			6.036		
S	1/3		1				1			1/3		

Table 10. Asymptotic values of the functions in the fundamental solutions of the fourth kind

r^*	$(C_n)_i R_n(r^*)$			$2(1 - r^*) (C_n)_i R_n'(1)$			$2(1 - r^*) (C_n)_o R_n'(r^*)$			$(C_n)_o R_n(1)$		
	K WKBJ	K Graph	S	K WKBJ	K Graph	S	K WKBJ	K Graph	S	K WKBJ	K Graph	S
0	0		0				∞			2.138		
0.02	1.133	0.0709	1.170	0.3407	0.0825	0.740	33.03	65.1	1.17	2.198	3.70	1.80
0.05	1.403	0.2065	1.282	0.6083	0.221	0.788	19.20	27.6	1.082	2.216	3.27	1.76
0.10	1.619	0.417	1.359	0.9360	0.458	0.836	12.89	17.3	1.07	1.230	2.99	1.73
0.2	1.826			1.426			8.736			2.237		
0.25	1.886	0.976	1.495	1.628	1.241	0.939	7.719	9.70	1.059	2.236	2.63	1.69
0.3	1.933			1.813			6.983			2.234		
0.4	2.001			2.144			5.963			2.226		
0.5	2.047	1.820	1.635	2.437	2.30	0.986	5.276	5.80	1.017	2.216	2.52	1.68
0.6	2.081			2.704			4.774			2.205		
0.7	2.108			2.950			4.386			2.193		
0.8	2.128			3.180			4.075			2.181		
1.0	2.148			3.601			3.601			2.148		
S	5/3		1				1			5/3		

used for the values of the eigen-constants which lie to the right of the intersection of the two lines in Fig. 1.[†]

The various fundamental solutions can now be constructed using (20). From this and the defining equations, the various non-dimensional quantities specified in [1] can be evaluated as functions of the axial position parameter, \bar{x} .

The $\theta_{ij}^{(k)}$ can be evaluated directly from (20) and we have, additionally, the relations

$$\Phi_{ij}^{(k)} = -2(1-r^*) \left[\frac{\partial \theta_{ij}^{(k)}}{\partial \bar{x}} \right]_{r=r^*} \quad (44)$$

$$\Phi_{oj}^{(k)} = 2(1-r^*) \left[\frac{\partial \theta_{oj}^{(k)}}{\partial \bar{x}} \right]_{r=r^*} \quad (45)$$

and

$$\theta_{mj}^{(k)} = \frac{4}{1+r^*} \int_0^{\bar{x}} [r^* \Phi_{ij}^{(k)} + \Phi_{oj}^{(k)}] d\bar{x}. \quad (46)$$

These parameters are related to the conventional Nusselt modulus by

$$Nu_{ij}^{(k)} = \frac{\Phi_{ij}^{(k)}}{[\theta_{ij}^{(k)} - \theta_{mj}^{(k)}]} \quad (47)$$

The values of these quantities are presented in Tables 11-18 and are plotted in Figs. 2-13.

[†] It is interesting to compare the WKBJ approximations with the values presented by Hatton and Quarmby [16] who obtained the first ten eigenvalues and constants. For $r^* = 0.5$ we have:

	Hatton and Quarmby	WKBJ
$(\lambda_g)_i^{(3)}$	61.73	61.8
$2(1-r^*)(C_g)_i^{(3)} R_g'(r^*)$	-1.592	1.58

As is indicated by equation (20), the values of interest at any axial station, \bar{x} , are obtained by adding or subtracting the series of the eigenfunctions to the fully established or terminal values. In all the cases where $\bar{x} > 1.0$ the terminal values have (or very nearly have) been obtained. As \bar{x} diminishes, the series represents a progressively greater part of the local value. Since the series contains an exponential term, $e^{-\lambda \bar{x}^2}$, the larger values of \bar{x} receive only the contribution of the first few terms, which are known very precisely from the machine calculation. For values of $\bar{x} = 0.01$, however, the higher terms (those beyond $n = 3$ or 4 in the present case) have begun to contribute. These terms, obtained from the graphical method and from the asymptotic (large λ) solutions, are known only to 1 or 2 per cent and, accordingly, the level of confidence in the values of the fundamental solutions diminishes with \bar{x} .

Those quantities which start from zero at $\bar{x} = 0$ and increase to their terminal values somewhere downstream are particularly affected by this uncertainty since, for small values of \bar{x} , the absolute values of these quantities are provided by the differences of nearly equal quantities and the uncertainty in the series represents a large fraction of the residual values.

Fortunately, the physical nature of the problem provides some internal checks on the accuracy, i.e. for small \bar{x} , $\Phi_{ij}^{(1)}$ approaches $\Phi_{ij}^{(0)}$, $\theta_{ij}^{(1)}$ approaches $\theta_{ij}^{(0)}$, etc. From these considerations it appears that the values of the series used for the wall values at $\bar{x} = 10^{-4}$ are within ± 1 per cent of the actual or correct values. At

Table 11. The fundamental solutions of the first kind temperature step at the inner wall

r^*	\bar{x}	$\Phi_{n1}^{(1)}$	$\Phi_{nj}^{(1)}$	$\theta_{nj1}^{(1)}$	$Nu_{nj1}^{(1)}$	$Nu_{nj2}^{(1)}$
0.02	0.0001	78.5	—	0.0011	78.6	—
	0.001	50.87	—	0.00523	51.2	—
	0.0025	43.77	—	0.01070	44.20	—
	0.005	39.28	—	0.01877	40.03	—
	0.01	35.47	-0.00143	0.03332	36.70	0.0430
	0.025	31.20	-0.06959	0.07048	33.57	0.9873
	0.05	28.38	-0.2408	0.1129	31.99	2.132
	0.1	26.12	-0.4162	0.1514	30.78	2.747
	0.25	25.08	-0.4981	0.1693	30.20	2.941
	∞	25.05	-0.5010	0.1699	30.18	2.947

Table 11—continued

r^*	\bar{x}	$\Phi_{ii}^{(1)}$	$\Phi_{oi}^{(1)}$	$\theta_{mi}^{(1)}$	$Nu_{ii}^{(1)}$	$Nu_{oi}^{(1)}$
0.05	0.0001	52.0	—	0.0014	52.1	—
	0.001	30.44	—	0.0076	30.67	—
	0.0025	25.19	—	0.01539	25.59	—
	0.005	22.03	—	0.02652	22.63	—
	0.01	19.39	-0.00247	0.04606	20.33	0.0536
	0.025	16.52	-0.1018	0.09426	18.24	1.080
	0.05	14.67	-0.3290	0.1468	17.19	2.241
	0.1	13.26	-0.5437	0.1914	16.40	2.840
	0.25	12.70	-0.6319	0.2096	16.06	3.014
	∞	12.68	-0.6342	0.2100	16.05	3.018
0.1	0.0001	40.4	—	0.0022	40.4	—
	0.001	21.95	—	0.0110	22.19	—
	0.0025	17.62	—	0.0215	18.01	—
	0.005	15.04	—	0.0362	15.60	—
	0.01	12.918	-0.00303	0.0613	13.76	0.0641
	0.025	10.651	-0.1409	0.1212	12.12	1.162
	0.05	9.227	-0.4306	0.1838	11.30	2.342
	0.1	8.198	-0.6860	0.2338	10.70	2.933
	0.25	7.824	-0.7798	0.2521	10.46	3.092
	∞	7.817	-0.7817	0.2525	10.45	3.095
0.25	0.0001	31.9	—	0.0038	32.1	—
	0.001	15.84	—	0.0183	16.1	—
	0.0025	12.14	—	0.0346	12.57	—
	0.005	9.978	—	0.0564	10.57	—
	0.01	8.238	-0.00763	0.0923	9.075	0.0827
	0.025	6.421	-0.2242	0.1735	7.769	1.292
	0.05	5.314	-0.6398	0.2533	7.118	2.525
	0.1	4.566	-0.9744	0.3123	6.640	3.120
	0.25	4.331	-1.080	0.3309	6.473	3.265
	∞	4.328	-1.082	0.3312	6.471	3.267
0.5	0.0001	28.3	—	0.0058	28.5	—
	0.001	13.34	—	0.0266	13.70	—
	0.0025	9.916	—	0.0492	10.43	—
	0.005	7.930	—	0.0784	8.605	—
	0.01	6.340	-0.0116	0.1251	7.247	0.0928
	0.025	4.697	-0.3212	0.2267	6.074	1.417
	0.05	3.713	-0.8845	0.3225	5.481	2.742
	0.1	3.072	-0.1315	0.3901	5.038	3.372
	0.25	2.887	-0.1441	0.4097	4.892	3.517
	∞	2.885	-0.1442	0.4099	4.890	3.518
1.0	0.00025	19.1	—	0.0145	19.4	—
	0.0025	8.64	—	0.0660	9.25	—
	0.01	5.242	-0.0170	0.1624	6.259	0.105
	0.025	3.687	-0.4571	0.2858	5.163	1.599
	0.05	2.761	-1.242	0.3992	4.597	3.111
	0.075	2.357	-1.642	0.4526	4.306	3.629
	0.10	2.168	-1.831	0.4777	4.151	3.834
	0.250	2.001	-1.998	0.4997	4.001	3.998
	∞	2.000	-2.000	0.5000	4.000	4.000

Table 12. The fundamental solutions of the first kind temperature step at the outer wall

r^*	\bar{x}	$\Phi_{m\alpha}^{(1)}$	$\Phi_{i\alpha}^{(1)}$	$\theta_{m\alpha}^{(1)}$	$Nu_{m\alpha}^{(1)}$	$Nu_{i\alpha}^{(1)}$
0.02	0.0001	23.0	..	0.015	23.3	..
	0.001	9.961	..	0.062	10.6	..
	0.0025	6.996	..	0.110	7.862	..
	0.005	5.270	..	0.169	6.341	..
	0.01	3.880	-0.146	0.2566	5.220	0.467
	0.025	2.434	-3.545	0.4324	4.288	8.199
	0.05	1.537	-12.08	0.6053	3.895	19.69
	0.1	8.346	-20.82	0.7573	3.439	27.50
	0.25	5.123	-24.90	0.8275	2.971	30.09
	∞	5.010	-25.05	0.8300	2.947	30.18
0.05	0.0001	23.3	..	0.014	23.6	..
	0.001	10.1	..	0.060	10.8	..
	0.0025	7.103	..	0.108	7.962	..
	0.005	5.355	..	0.1669	6.420	..
	0.01	3.951	-0.0419	0.2525	5.286	0.166
	0.025	2.491	-2.0299	0.4261	4.341	4.763
	0.05	1.590	-6.577	0.5933	3.910	11.08
	0.1	0.9151	-10.87	0.7319	3.413	14.85
	0.25	0.6414	-12.63	0.7884	3.031	16.03
	∞	0.6342	-12.68	0.7899	3.018	16.05
0.1	0.0001	23.6	..	0.013	23.9	..
	0.001	10.27	..	0.058	10.9	..
	0.0025	7.227	..	0.104	8.070	..
	0.005	5.461	..	0.161	6.508	..
	0.01	4.044	-0.0379	0.2453	5.358	0.154
	0.025	2.571	-1.408	0.4148	4.394	3.394
	0.05	1.669	-4.306	0.5148	3.927	7.490
	0.1	1.021	-6.859	0.7005	3.413	9.791
	0.25	0.7865	-7.779	0.7465	3.102	10.44
	∞	0.7817	-7.817	0.7474	3.095	10.45
0.25	0.0001	24.1	..	0.01176	24.4	..
	0.001	10.61	..	0.053	11.20	..
	0.0025	7.514	..	0.095	1.300	..
	0.005	5.717	..	0.144	6.698	..
	0.01	4.277	-0.9292	0.225	5.517	0.1301
	0.025	2.786	-0.8961	0.3827	4.513	2.341
	0.05	1.884	-2.559	0.5283	3.995	4.843
	0.1	1.276	-3.897	0.6347	3.493	6.140
	0.25	1.084	-4.321	0.6683	3.270	6.466
	∞	1.082	-4.328	0.6688	3.267	6.471
0.5	0.0001	25.0	..	0.0098	25.2	..
	0.001	11.08	..	0.045	11.6	..
	0.0025	7.919	..	0.082	8.627	..
	0.005	6.086	..	0.128	6.978	..
	0.01	4.621	-0.0232	0.198	5.760	0.117
	0.025	3.108	-0.6424	0.3407	4.716	1.835
	0.05	2.203	-1.769	0.4714	4.169	3.752
	0.1	1.615	-2.631	0.5631	3.696	4.672
	0.25	1.444	-2.882	0.5897	3.521	4.888
	∞	1.442	-2.885	0.5900	3.518	4.890

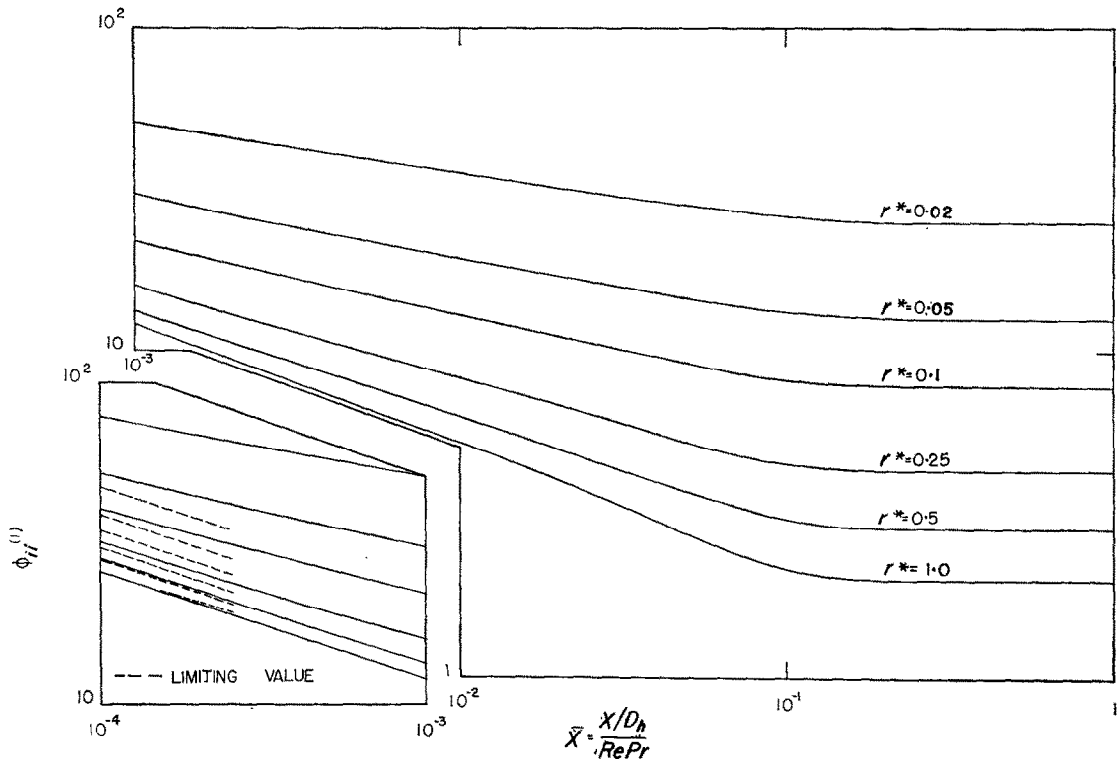


FIG. 2. Inner wall heat flux functions for the fundamental solutions of the first kind.

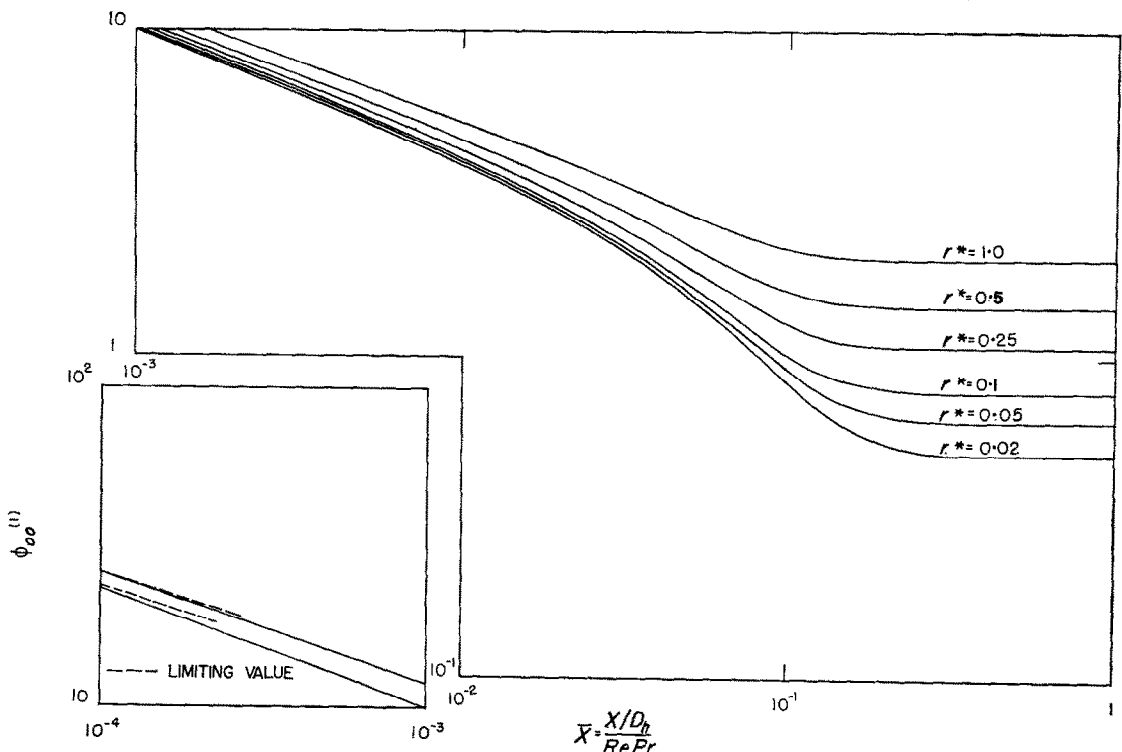


FIG. 3. Outer wall heat fluxes for the fundamental solutions of the first kind.

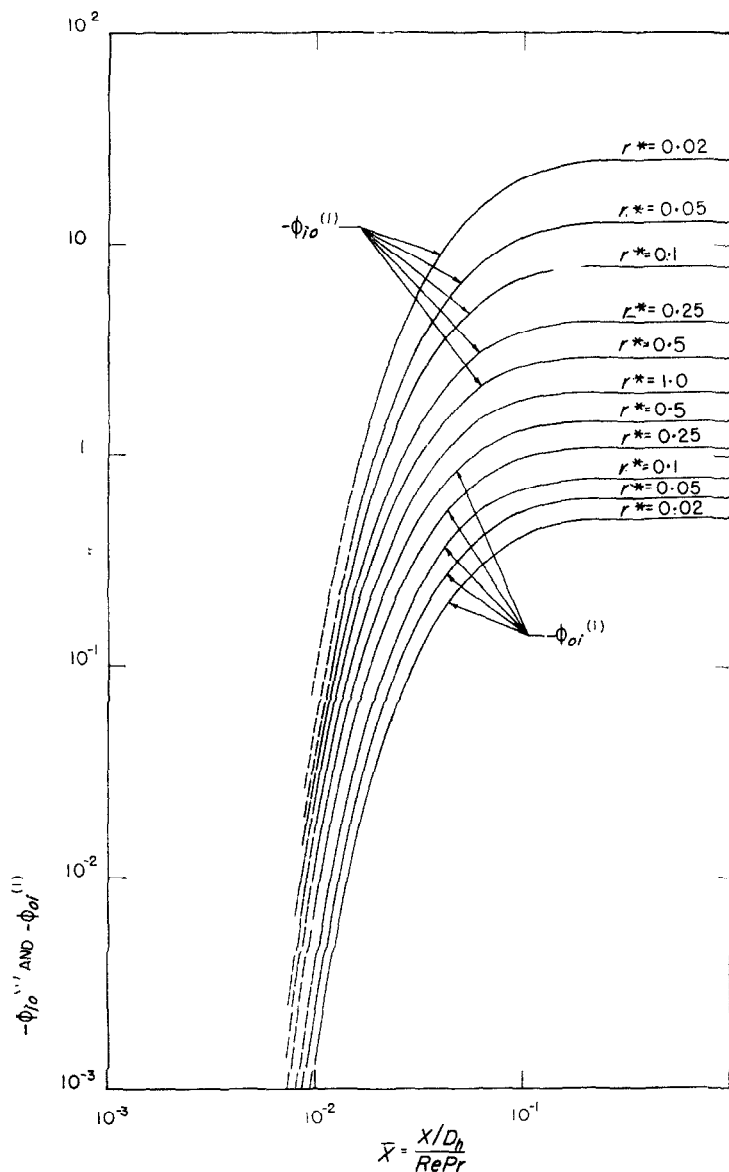


FIG. 4. Induced heat fluxes for the fundamental solutions of the first kind.

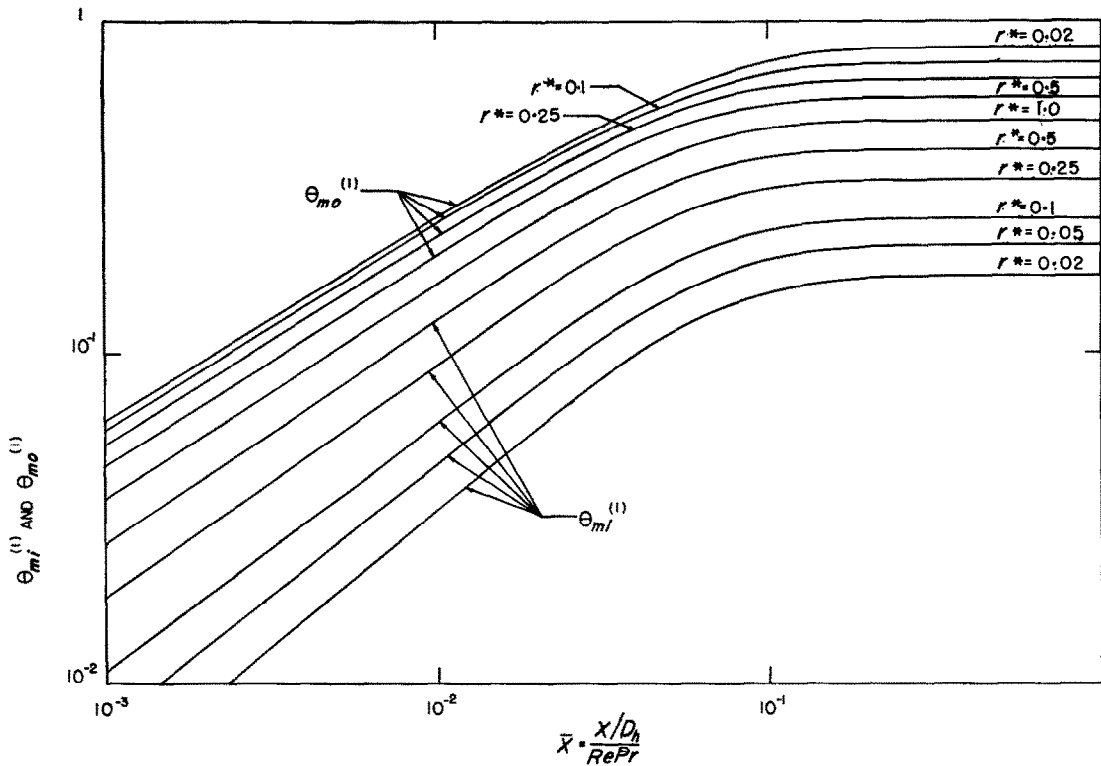


FIG. 5. Mean temperatures for the fundamental solutions of the first kind.

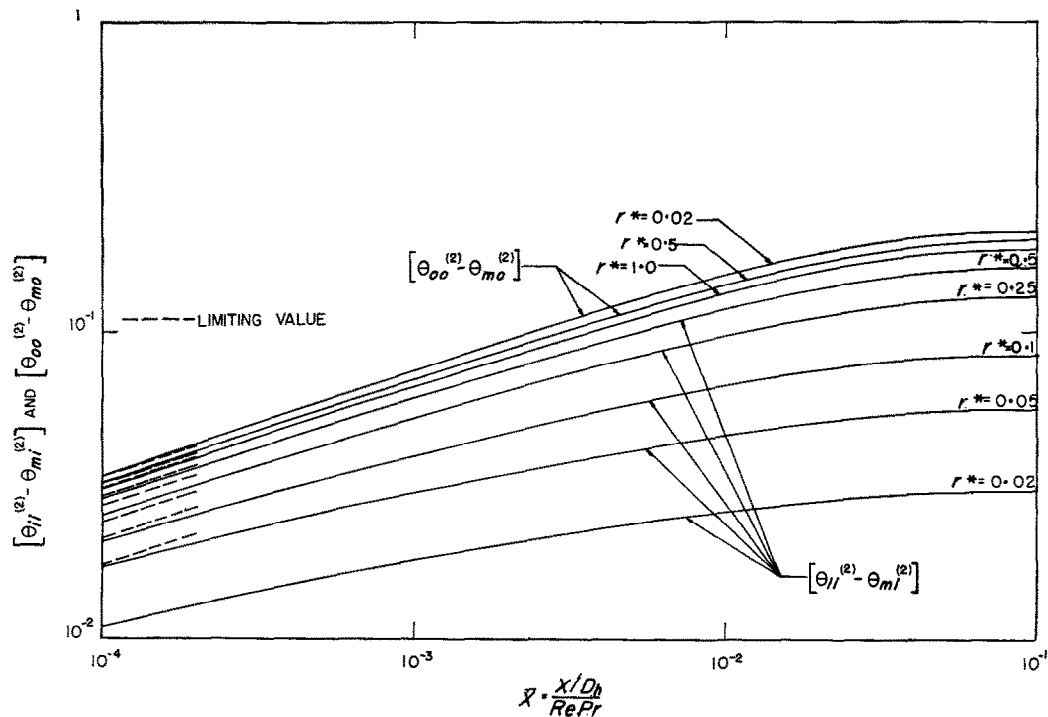


FIG. 6. Wall temperature differences for the fundamental solutions of the second kind.

Table 13. The fundamental solutions of the second kind inner wall heated

r^*	\bar{x}	$[\theta_{ii}^{(2)} - \theta_{mi}^{(2)}]$	$[\theta_{mi}^{(2)} - \theta_{mi}^{(2)}]$	$\theta_{mi}^{(2)}$	$Nu_{ii}^{(2)}$
0.02	0.0001	0.0109	-0.0 ₅ 7843	0.0 ₅ 7843	91.9
	0.001	0.0182	-0.0 ₄ 7843	0.0 ₄ 7843	54.8
	0.0025	0.02145	-0.0 ₃ 1960	0.0 ₃ 1960	46.63
	0.005	0.02389	-0.0 ₃ 3921	0.0 ₃ 3921	41.86
	0.010	0.02625	-0.0 ₃ 7843	0.0 ₃ 7843	38.09
	0.025	0.02893	-0.001726	0.001960	34.55
	0.05	0.03018	0.002354	0.003921	33.12
	0.10	0.03055	-0.002547	0.007843	32.72
	0.25	0.03057	-0.002558	0.01960	32.70
	∞	0.03057	-0.002558	∞	32.70
0.05	0.0001	0.0172	-0.0 ₄ 1904	0.0 ₄ 1904	58.0
	0.0010	0.0301	-0.0 ₃ 1904	0.0 ₃ 1904	33.2
	0.0025	0.03626	-0.0 ₃ 4761	0.0 ₃ 4761	27.58
	0.0050	0.04132	-0.0 ₃ 9523	0.0 ₃ 9523	24.20
	0.0100	0.04646	-0.001899	0.001904	21.52
	0.025	0.05246	0.004166	0.004761	19.06
	0.050	0.05527	0.005652	0.009523	18.09
	0.10	0.05609	-0.006101	0.01904	17.82
	0.25	0.05614	-0.006128	0.04761	17.81
	∞	0.05614	-0.006128	∞	17.81
0.10	0.0001	0.0207	-0.0 ₄ 3636	0.0 ₄ 3636	48.3
	0.0010	0.0399	-0.0 ₃ 3636	0.0 ₃ 3636	25.1
	0.0025	0.04999	-0.0 ₃ 9090	0.0 ₃ 9090	20.01
	0.0050	0.05842	-0.001818	0.001818	17.12
	0.010	0.06710	-0.003624	0.003636	14.90
	0.025	0.07749	-0.007918	0.009090	12.90
	0.05	0.08245	0.01071	0.01818	12.12
	0.10	0.08390	0.01156	0.03636	11.91
	0.25	0.08399	0.01162	0.09090	11.90
	∞	0.08399	-0.01162	∞	11.90
0.25	0.0001	0.0253	0.0 ₄ 8000	0.0 ₄ 8000	39.5
	0.0010	0.0530	0.0 ₃ 8000	0.0 ₃ 8000	18.9
	0.0025	0.06887	-0.002000	0.002000	14.52
	0.0050	0.08280	-0.003966	0.004000	12.08
	0.010	0.09779	-0.007936	0.008000	10.22
	0.025	0.11662	-0.01731	0.02000	8.574
	0.05	0.12596	-0.02347	0.04000	7.938
	0.10	0.12879	-0.02539	0.08000	7.764
	0.25	0.12897	-0.02552	0.2000	7.753
	∞	0.12897	-0.02552	∞	7.753
0.05	0.0001	0.0289	0.0 ₃ 1333	0.0 ₃ 1333	34.6
	0.0010	0.0611	-0.0 ₂ 1333	0.0 ₂ 1333	16.4
	0.0025	0.0809	-0.0 ₂ 3333	0.0 ₂ 3333	12.37
	0.0050	0.0987	-0.0 ₂ 6666	0.0 ₂ 6666	10.13
	0.010	0.1185	-0.01328	0.013333	8.433
	0.025	0.1442	0.02888	0.033333	6.931
	0.05	0.1574	-0.03922	0.066667	6.353
	0.10	0.1615	-0.04253	0.13333	6.192
	0.25	0.1617	-0.04275	0.33333	6.181
	∞	0.1617	-0.04275	∞	6.181

Table 13—continued

r^*	\bar{x}	$[\theta_{ti}^{(2)} - \theta_{mi}^{(2)}]$	$[\theta_{oi}^{(2)} - \theta_{mi}^{(2)}]$	$\theta_{mi}^{(2)}$	$Nu_{ti}^{(2)}$
1.0	0.00025	0.0425	-0.0005	0.0005	23.5
	0.0025	0.893	-0.005	0.005	11.2
	0.01	0.1335	-0.01992	0.02	7.489
	0.025	0.1643	-0.04330	0.05	6.085
	0.05	0.1803	-0.05888	0.1	5.546
	0.075	0.1843	-0.06290	0.15	5.424
	0.25	0.1857	-0.06428	0.5	5.384
	∞	0.1857	-0.06428	∞	5.384

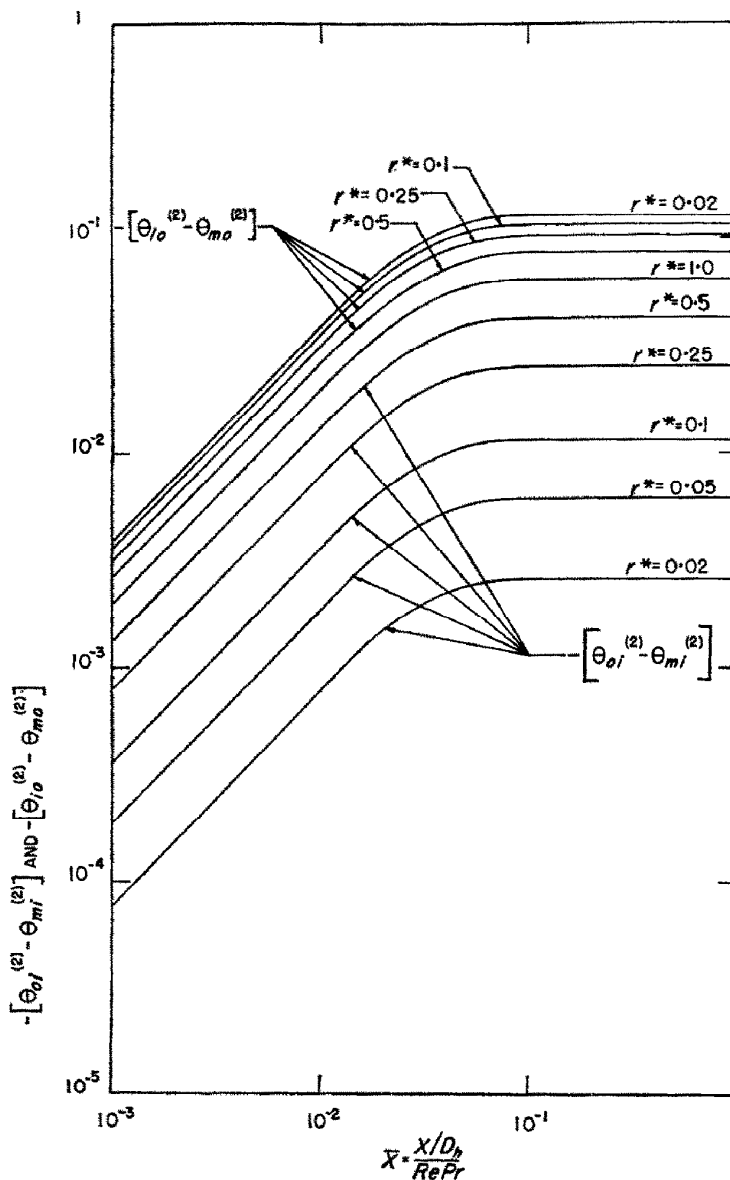


FIG. 7. Induced temperature differences for the fundamental solutions of the second kind.

Table 14. The fundamental solutions of the second kind outer wall heated

r^*	\bar{x}	$[\theta_{m0}^{(2)} - \theta_{m0}^{(2)}]$	$[\theta_{m0}^{(2)} - \theta_{m0}^{(2)}]$	$\theta_{m0}^{(2)}$	$Nu_{m0}^{(2)}$
0.02	0.0001	0.0341	-0.03921	0.03921	29.3
	0.001	0.07560	-0.003921	0.003921	13.2
	0.0025	0.1022	-0.008903	0.009803	9.784
	0.005	0.1266	-0.01907	0.01907	7.898
	0.010	0.1538	-0.03909	0.03921	6.501
	0.025	0.1886	-0.08632	0.09803	5.299
	0.05	0.2058	-0.1177	0.1960	4.857
	0.10	0.2109	-0.1273	0.3921	4.741
	0.25	0.2112	-0.1279	0.9803	4.734
	∞	0.2112	-0.1279	∞	4.734
0.05	0.0001	0.0337	-0.03809	0.03809	29.7
	0.0010	0.0748	-0.003809	0.003809	13.4
	0.0025	0.1011	-0.009523	0.009523	9.895
	0.005	0.1252	-0.01903	0.01904	7.991
	0.010	0.1520	-0.03798	0.03809	6.577
	0.025	0.1865	-0.08332	0.09523	5.361
	0.050	0.2034	-0.1130	0.1904	4.915
	0.10	0.2083	-0.1220	0.3809	4.798
	0.25	0.2086	-0.1225	0.9523	4.791
	∞	0.2086	-0.1225	∞	4.791
0.1	0.0001	0.0334	-0.03636	0.03636	29.9
	0.00025	0.0461	-0.03909	0.03909	21.7
	0.0005	0.0586	-0.001818	0.001818	17.1
	0.001	0.07406	-0.003636	0.003636	13.50
	0.0025	0.09991	-0.009090	0.009090	10.1
	0.005	0.1237	-0.01817	0.01818	8.083
	0.010	0.1503	-0.03624	0.03636	6.651
	0.025	0.1846	-0.07918	0.09090	5.416
	0.05	0.2015	-0.1071	0.1818	4.960
	0.10	0.2065	-0.1156	0.3636	4.841
0.25	0.2068	-0.1162	0.9090	4.834	
	∞	0.2068	-0.1162	∞	4.834
0.25	0.0001	0.0331	-0.03200	0.03200	30.2
	0.0010	0.07248	-0.003200	0.003200	13.80
	0.0025	0.09760	-0.008000	0.008000	10.25
	0.0050	0.1208	-0.016000	0.01600	8.275
	0.010	0.1470	-0.03188	0.03200	6.802
	0.025	0.1811	-0.06940	0.08000	5.521
	0.050	0.1983	-0.09404	0.1600	5.042
	0.10	0.2035	-0.1017	0.3200	4.912
	0.25	0.2038	-0.1022	0.8000	4.904
	∞	0.2038	-0.1023	∞	4.904
0.5	0.0001	0.0325	-0.032666	0.032666	30.8
	0.001	0.07039	-0.002666	0.002666	14.21
	0.0025	0.09457	-0.006666	0.006666	10.57
	0.005	0.1170	-0.01333	0.01333	8.547
	0.010	0.1423	-0.02656	0.02666	7.026
	0.025	0.1756	-0.05676	0.06666	5.693
	0.05	0.1928	-0.07844	0.1333	5.186
	0.10	0.1981	-0.08506	0.2666	5.045
	0.25	0.1985	-0.08551	0.6666	5.036
	∞	0.1985	-0.08551	∞	5.036

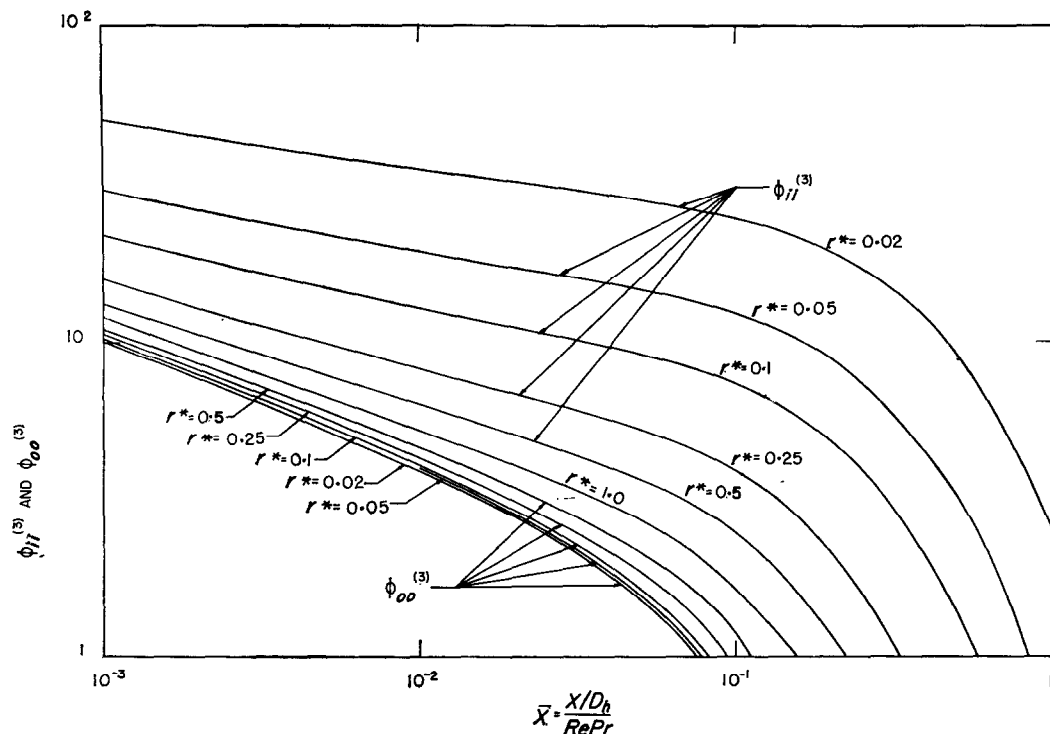


FIG. 8. Heat fluxes for the fundamental solutions of the third kind.

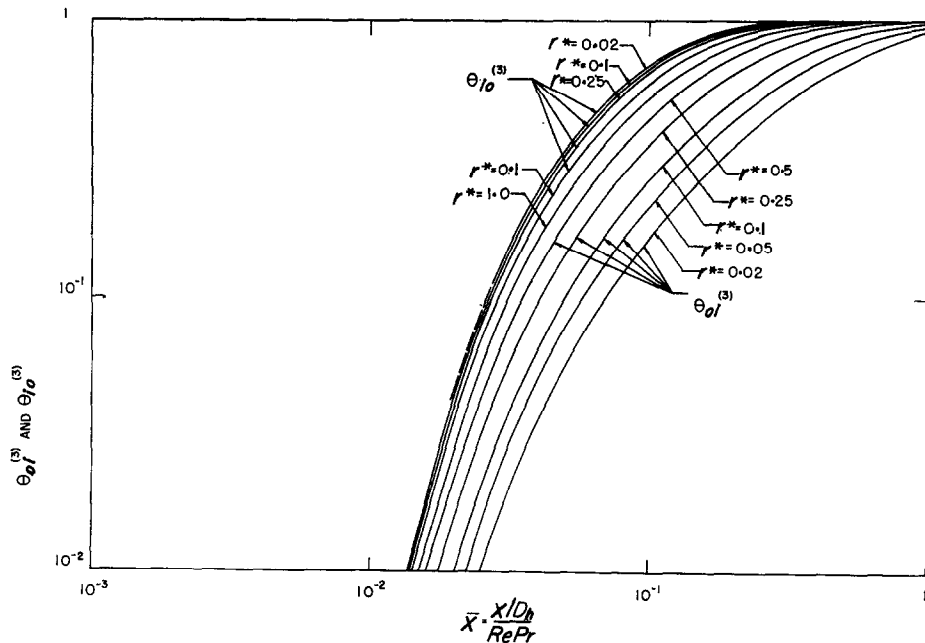


FIG. 9. Induced temperatures for the fundamental solutions of the third kind.

Table 15. The fundamental solutions of the third kind temperature step at the inner wall

r^*	\bar{x}	$\Phi_{\alpha}^{(3)}$	$\theta_{\alpha i}^{(3)}$	$\theta_{mi}^{(3)}$	$Nu_{\alpha i}^{(3)}$
0.02	0.0001	78.0	—	0.001	78.4
	0.001	50.71	—	0.0052	51.2
	0.0025	43.62	—	0.0105	44.28
	0.005	39.19	—	0.0186	40.12
	0.01	35.39	0.03116	0.0331	36.77
	0.025	31.12	0.01019	0.0739	33.69
	0.05	28.20	0.05729	0.1340	32.57
	0.1	24.66	0.1669	0.2374	32.34
	0.25	16.85	0.4305	0.4787	32.33
	∞	0.0	1.0000	1.0000	32.33
0.05	0.0001	51.5	—	0.0012	51.5
	0.001	30.30	—	0.0072	30.5
	0.0025	25.16	—	0.0149	25.55
	0.005	22.03	—	0.0261	22.62
	0.01	19.40	0.03195	0.0456	20.33
	0.025	16.52	0.01488	0.0962	18.28
	0.05	14.60	0.07800	0.1698	17.59
	0.1	12.27	0.2167	0.2972	17.46
	0.25	7.451	0.5243	0.5732	17.46
	∞	0.0	1.0000	1.0000	17.46
0.1	0.0001	40.4	—	0.0021	40.4
	0.001	21.94	—	0.0109	22.2
	0.025	17.61	—	0.0214	18.00
	0.005	15.04	—	0.0361	15.60
	0.01	12.920	0.03320	0.0612	13.76
	0.025	10.652	0.02049	0.1244	12.16
	0.05	9.160	0.1012	0.2136	11.64
	0.1	7.365	0.2691	0.3629	11.56
	0.25	3.920	0.6109	0.6609	11.56
	∞	0.0	1.0000	1.0000	11.56
0.25	0.0001	31.9	—	0.0038	32.0
	0.001	15.82	—	0.0183	16.11
	0.0025	12.13	—	0.0346	12.56
	0.005	9.976	—	0.0564	10.47
	0.01	8.238	0.03575	0.0923	9.075
	0.025	6.420	0.03177	0.1781	7.812
	0.05	5.248	0.1449	0.2934	7.428
	0.1	3.876	0.3610	0.4741	7.371
	0.25	1.600	0.7361	0.7828	7.370
	∞	0.0	1.0000	1.0000	7.370
0.5	0.0001	28.2	—	0.0057	28.4
	0.001	13.32	—	0.0265	13.68
	0.0025	9.909	—	0.0490	10.42
	0.005	7.929	—	0.0782	8.602
	0.01	6.3407	0.03871	0.1250	7.246
	0.025	4.6968	0.04351	0.2322	6.117
	0.05	3.6492	0.1880	0.3692	5.785
	0.1	2.4675	0.4440	0.5700	5.738
	0.25	0.7830	0.8235	0.8635	5.738
	∞	0.0	1.0000	1.0000	5.738

Table 15—continued

r^*	\tilde{x}	$\Phi_{tt}^{(3)}$	$\theta_{oi}^{(3)}$	$\theta_{mi}^{(3)}$	$Nu_{ti}^{(3)}$
1.00	0.0025	8.64	—	0.0660	9.25
	0.01	5.242	0.00119	0.1625	6.259
	0.025	3.6868	0.05685	0.2919	5.206
	0.05	2.7028	0.2356	0.4486	4.902
	0.075	2.1021	0.3981	0.5680	4.866
	0.25	0.3830	0.8901	0.9211	4.860
	∞	0.0	1.0000	1.0000	4.860

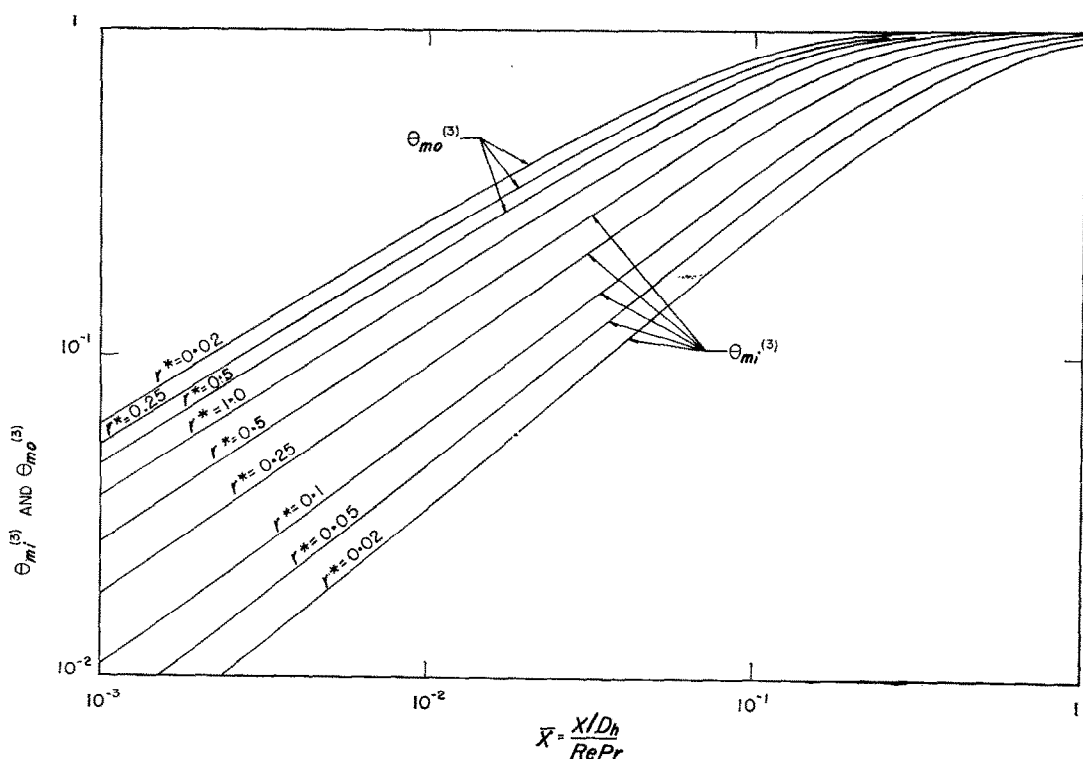


FIG. 10. Mean temperatures for the fundamental solutions of the third kind.

Table 16. The fundamental solutions of the third kind temperature step at the outer wall

r^*	\tilde{x}	$\theta_{in}^{(3)}$	$\Phi_{in}^{(3)}$	$\theta_{mu}^{(3)}$	$Nu_{mu}^{(3)}$
0.02	0.0001	—	23.2	0.013	23.5
	0.001	—	10.1	0.061	10.8
	0.0025	—	7.049	0.109	7.914
	0.005	—	5.280	0.16	6.350
	0.01	0.00118	3.881	0.2562	5.217
	0.025	0.08227	2.434	0.4336	4.298
	0.05	0.3427	1.524	0.6219	4.031
	0.1	0.6972	0.6889	0.8275	3.994
	0.25	0.9710	0.06575	0.9835	3.993
	∞	1.0	0.0	1.0000	3.993
0.05	0.0001	—	23.4	0.013	23.7
	0.001	—	10.20	0.060	10.9
	0.0025	—	7.139	0.108	8.000
	0.005	—	5.362	0.166	6.428
	0.01	0.00140	3.951	0.2525	5.286
	0.025	0.08435	2.491	0.4285	4.359
	0.05	0.3431	1.570	0.6163	4.093
	0.1	0.6944	0.7176	0.8231	4.057
	0.25	0.9699	0.07066	0.9825	4.056
	∞	1.0000	0.0	1.0000	4.056
0.1	0.0001	—	23.7	0.013	24.0
	0.001	—	10.33	0.058	11.00
	0.0025	—	7.251	0.104	8.095
	0.005	—	5.465	0.161	6.513
	0.01	0.00153	4.044	0.2453	5.359
	0.025	0.0840	2.571	0.4180	4.418
	0.05	0.3369	1.642	0.6041	4.149
	0.1	0.6840	0.7696	0.8129	4.114
	0.25	0.9664	0.08162	0.9801	4.113
	∞	1.0000	0.0	1.0000	4.113
0.25	0.0001	—	24.2	0.012	24.5
	0.001	—	10.6	0.053	11.2
	0.0025	—	7.524	0.095	8.311
	0.005	—	5.718	0.147	6.700
	0.01	0.00159	4.277	0.2248	5.517
	0.025	0.0785	2.785	0.3873	4.547
	0.05	0.3129	1.845	0.5678	4.269
	0.1	0.6488	0.9280	0.7807	4.232
	0.25	0.9539	0.1217	0.9712	4.232
	∞	1.0000	0.0	1.0000	4.232
0.5	0.0001	—	24.9	0.010	25.1
	0.001	—	11.1	0.045	11.6
	0.0025	—	7.920	0.082	8.629
	0.005	—	6.086	0.128	6.980
	0.01	0.001467	4.621	0.198	5.761
	0.025	0.0693	3.108	0.3466	4.757
	0.05	0.2796	2.153	0.5180	4.468
	0.1	0.5988	1.181	0.7333	4.429
	0.25	0.9317	0.2008	0.9546	4.429
	∞	1.0000	0.0	1.0000	4.429

Table 17. The fundamental solutions of the fourth kind inner wall heated

r^*	\bar{x}	$\theta_{ei}^{(4)}$	$\Phi_{oi}^{(4)}$	$\theta_{mi}^{(4)}$	$Nu_{ei}^{(4)}$	$Nu_{oi}^{(4)}$
0.02	0.0001	0.0103	—	0.0 ₅ 7848	97.3	—
	0.001	0.0181	—	0.0 ₄ 7843	55.4	—
	0.0025	0.02159	—	0.0 ₁ 960	46.75	—
	0.005	0.02427	—	0.0 ₃ 3921	41.88	—
	0.01	0.02703	-0.0 ₄ 238	0.0 ₃ 7843	38.09	0.0302
	0.025	0.03090	-0.001645	0.001926	34.51	0.8541
	0.05	0.03406	-0.006855	0.003470	32.69	1.975
	0.1	0.03725	-0.01394	0.005268	31.26	2.646
	0.25	0.03966	-0.01942	0.006640	30.28	2.924
	∞	0.03991	-0.02000	0.006785	30.18	2.947
0.05	0.0001	0.0160	—	0.0 ₁ 904	62.4	—
	0.001	0.0298	—	0.0 ₃ 1904	33.8	—
	0.0025	0.03658	—	0.0 ₃ 4761	27.70	—
	0.005	0.04253	—	0.0 ₃ 9523	24.21	—
	0.01	0.04837	-0.0 ₄ 696	0.001904	21.52	0.0365
	0.25	0.05722	-0.004218	0.004671	19.02	0.9028
	0.05	0.06467	-0.01715	0.008415	17.77	2.038
	0.1	0.07232	-0.03472	0.01279	16.79	2.713
	0.25	0.07819	-0.04849	0.01619	16.12	2.995
	∞	0.07883	-0.05000	0.01656	16.05	3.018
0.1	0.0001	0.0195	—	0.0 ₄ 3636	51.5	—
	0.001	0.0399	—	0.0 ₃ 3636	25.3	—
	0.0025	0.05083	—	0.0 ₃ 9090	20.03	—
	0.005	0.06023	—	0.001818	17.12	—
	0.01	0.07074	-0.0 ₃ 152	0.003636	14.90	0.0418
	0.025	0.08658	-0.008401	0.008916	12.87	0.9422
	0.05	0.1003	-0.03368	0.01609	11.86	2.093
	0.1	0.1149	-0.06840	0.02462	11.07	2.777
	0.25	0.1265	-0.09664	0.03149	10.52	3.069
	∞	0.1279	-0.10000	0.03230	10.45	3.095
0.25	0.0001	0.0247	—	0.0 ₄ 8000	40.6	—
	0.001	0.0535	—	0.0 ₃ 8000	19.0	—
	0.0025	0.07081	—	0.002000	14.53	—
	0.005	0.08679	—	0.004000	12.08	—
	0.01	0.1058	-0.0 ₃ 397	0.007998	10.225	0.0497
	0.025	0.1366	-0.01961	0.01963	8.548	0.9989
	0.05	0.1654	-0.07824	0.03572	7.709	2.189
	0.1	0.1978	-0.1622	0.05780	7.040	2.908
	0.25	0.2266	-0.2384	0.07380	6.540	3.231
	∞	0.2310	-0.2500	0.07652	6.471	3.267
0.5	0.0001	0.0289	—	0.0 ₃ 1333	34.9	—
	0.001	0.0623	—	0.001333	16.41	—
	0.0025	0.0842	—	0.003333	12.38	—
	0.005	0.1054	—	0.006666	10.13	—
	0.01	0.1319	-0.0 ₃ 729	0.01333	8.437	0.0545
	0.025	0.1776	-0.03466	0.03285	6.908	1.055
	0.05	0.2232	-0.1398	0.06040	6.139	2.315
	0.1	0.2784	-0.2994	0.09680	5.505	3.093
	0.25	0.3349	-0.4658	0.1343	4.985	3.466
	∞	0.3465	-0.5000	0.1420	4.890	3.518

Table 17—continued

r^*	\bar{x}	$\theta_{ii}^{(4)}$	$\Phi_{oi}^{(4)}$	$\theta_{mi}^{(4)}$	$Nu_{ti}^{(4)}$	$Nu_{oi}^{(4)}$
1.0	0.00025	0.0430	—	0.0005	23.5	—
	0.0025	0.0943	—	0.0050	11.2	—
	0.01	0.1535	-0.001202	0.02000	7.489	0.0601
	0.025	0.2143	-0.05684	0.04934	6.061	1.152
	0.05	0.2793	-0.2356	0.09211	5.341	2.557
	0.075	0.3272	-0.3981	0.1261	4.971	3.156
	0.25	0.4684	-0.8901	0.2274	4.147	3.914
	∞	0.5000	-1.0000	0.2500	4.000	4.000

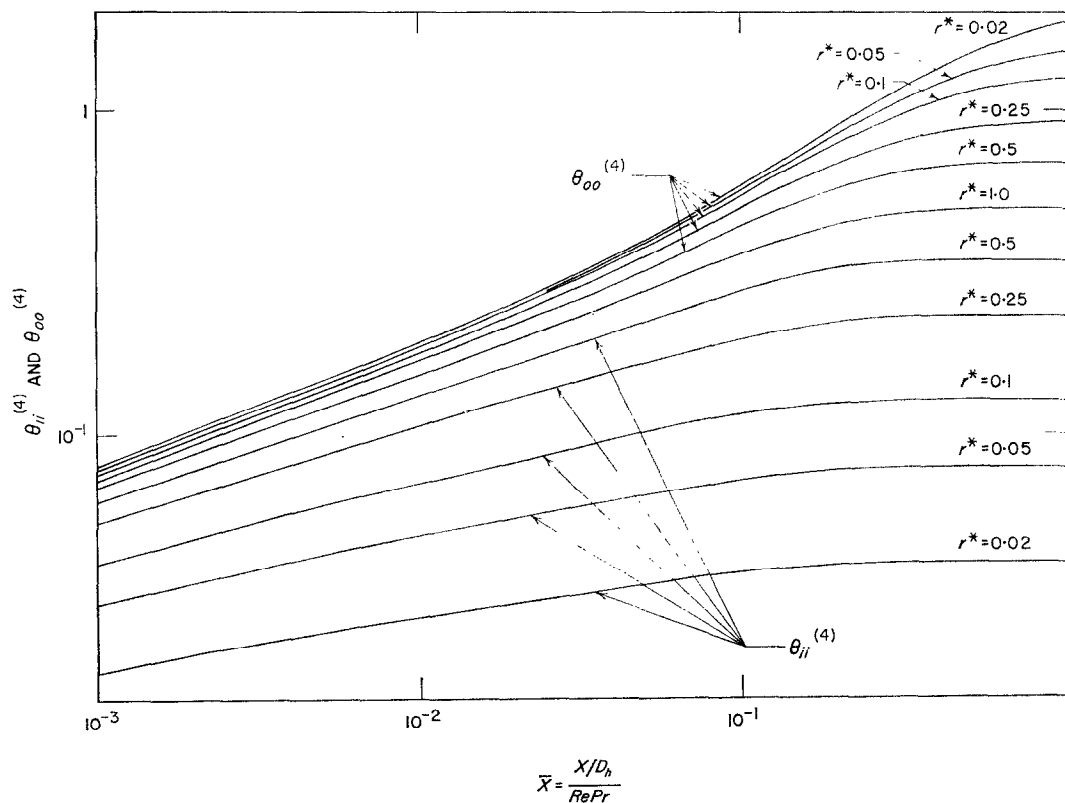


FIG. 11. Wall temperatures for the fundamental solutions of the fourth kind.

Table 18. The fundamental solutions of the fourth kind outer wall heated

r^*	\tilde{x}	$\theta_{00}^{(4)}$	$\Phi_{io}^{(4)}$	$\theta_{mo}^{(4)}$	$Nu_{00}^{(4)}$	$Nu_{io}^{(4)}$
0.02	0.0001	0.0375	—	0.03921	33.2	—
	0.001	0.08053	—	0.003921	14.37	—
	0.0025	0.1123	—	0.009803	10.47	—
	0.005	0.1463	—	0.01907	8.357	—
	0.01	0.1930	—	0.03921	6.808	—
	0.025	0.2867	-0.663	0.09803	5.489	6.34
	0.5	0.4017	-3.013	0.1960	4.937	15.12
	0.1	0.5934	-8.482	0.3726	4.529	22.76
	0.25	1.0373	-21.617	0.7789	3.871	27.75
	∞	1.9959	-50.000	1.656	2.947	30.18
0.05	0.0001	0.0366	—	0.03809	27.2	—
	0.001	0.0794	—	0.003809	13.1	—
	0.0025	0.1108	—	0.009523	9.817	—
	0.005	0.1442	—	0.01904	7.950	—
	0.01	0.1901	—	0.03750	6.552	—
	0.025	0.2817	-0.286	0.09438	5.337	3.03
	0.05	0.3934	-1.549	0.1854	4.807	8.355
	0.1	0.5760	-4.326	0.3477	4.379	12.44
	0.25	0.9691	-10.482	0.7003	3.720	14.96
	∞	1.5767	-20.000	1.2455	3.018	16.05
0.1	0.0001	0.0355	—	0.03636	28.3	—
	0.001	0.0782	—	0.003636	13.4	—
	0.0025	0.1091	—	0.009090	9.984	—
	0.005	0.1419	—	0.01818	8.074	—
	0.01	0.1867	—	0.03625	6.646	—
	0.025	0.2755	-0.2029	0.09040	5.401	2.244
	0.05	0.3827	-1.010	0.1760	4.835	5.738
	0.1	0.5536	-2.690	0.3237	4.349	8.309
	0.25	0.8930	-6.108	0.6195	3.656	9.860
	∞	1.2792	-10.000	0.9561	3.111	10.45
0.25	0.0001	0.0336	—	0.03200	30.0	—
	0.001	0.0758	—	0.003200	13.8	—
	0.0025	0.1056	—	0.008000	10.24	—
	0.005	0.1369	—	0.01600	8.27	—
	0.01	0.1790	—	0.03198	6.801	—
	0.025	0.2611	-0.1269	0.07941	5.504	1.598
	0.05	0.3574	-0.5796	0.1525	4.879	3.800
	0.1	0.5027	-1.444	0.2713	4.320	5.322
	0.25	0.7501	-2.944	0.4749	3.632	6.200
	∞	0.9242	-4.000	0.6181	3.267	6.471
0.5	0.0001	0.0322	—	0.032666	31.2	—
	0.001	0.0729	—	0.002666	14.2	—
	0.0025	0.1012	—	0.006666	10.56	—
	0.005	0.1303	—	0.01333	8.539	—
	0.01	0.1689	—	0.02654	7.020	—
	0.025	0.2423	-0.0869	0.06588	5.667	1.320
	0.05	0.3251	-0.3761	0.1249	4.995	3.010
	0.1	0.4425	-0.8881	0.2151	4.398	4.127
	0.25	0.6136	-1.647	0.3474	3.757	4.740
	∞	0.6931	-2.000	0.4089	3.518	4.890

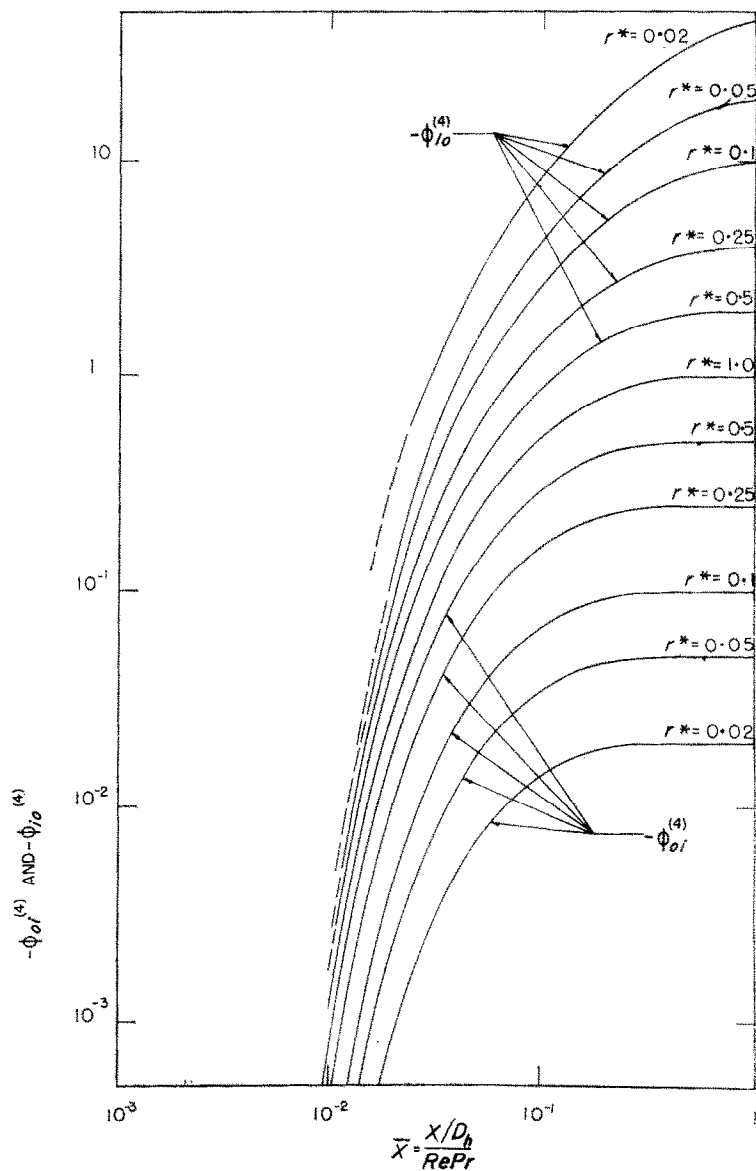


FIG. 12. Induced heat fluxes for the fundamental solutions of the fourth kind.

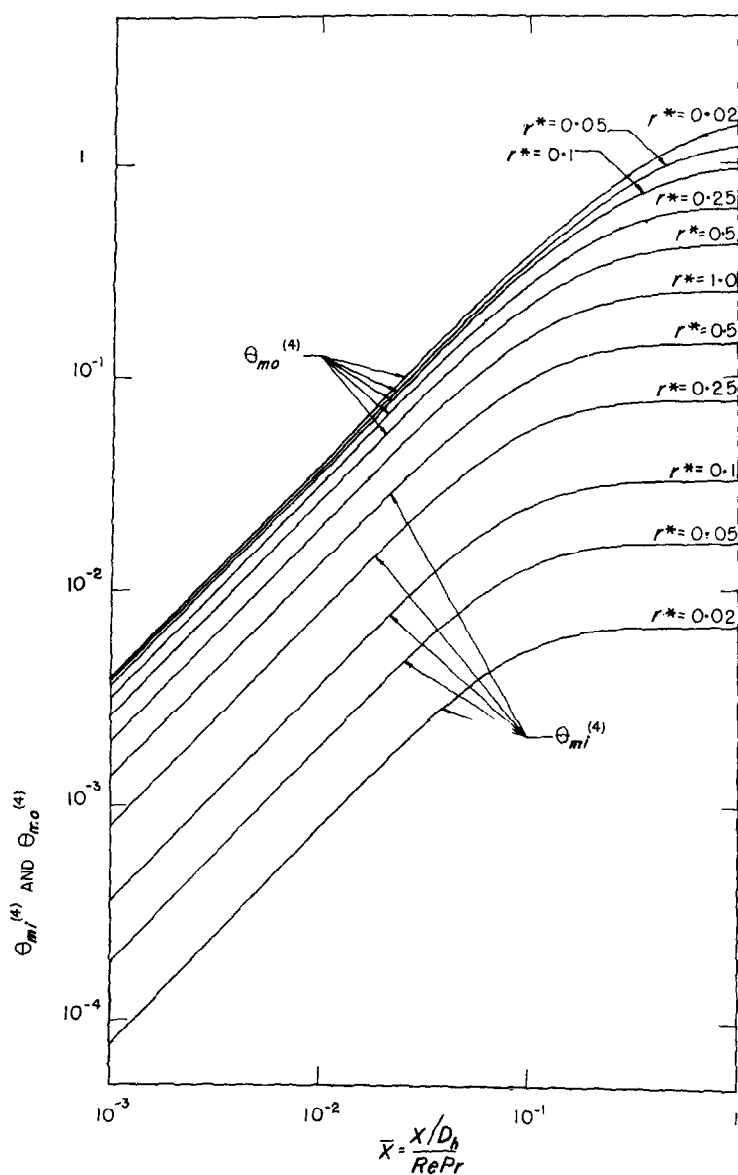


FIG. 13. Mean temperatures for the fundamental solutions of the fourth kind.

this value of \bar{x} , $\Phi_{ii}^{(1)}$ and $\Phi_{ii}^{(3)}$ are reliable to ± 1 per cent, and $\theta_{ii}^{(2)}$ and $\theta_{ii}^{(4)}$ are (because they have diminished in absolute value) reliable to ± 5 per cent.

The opposite wall values [e.g. $\theta_{oi}^{(2)}$] diminish rather rapidly and in all the cases for $\bar{x} > 0.01$ they are substantially zero (less than 0.1 per cent of terminal value).

For very small values of \bar{x} the Leveque approximations provide a good estimate for the applicable quantities. For all cases where the non-zero boundary condition is at the outer wall, and for the inner wall heated cases with $r^* \geq 0.5$, the Leveque solution agrees well with the computation at $\bar{x} = 10^{-1}$. For small values of r^* , when the heating is at the inner wall it appears that the approximate solution will not

become valid until \bar{x} is very small. For $r^* = 0.02$, $\bar{x} < 10^{-6}$ seems to be required, but for $r^* \geq 0.05$, $\bar{x} < 10^{-5}$ appears adequate.

This difficulty arises from the neglect of the curvature term in equation (1). For small values of r^* the depth of penetration of the temperature signal must be very small before this is justified.

COMPARISON WITH EXPERIMENT

The apparatus described in [1] was used to obtain the fundamental solutions of the second kind experimentally. The measured values of $\theta_{ii}^{(2)} - \theta_{mi}^{(2)}$ and $\theta_{oi}^{(2)} - \theta_{mo}^{(2)}$ are given in Figs. 14 and 15 together with the theoretical values.

The values of r^* that were used for the inner wall heated experiments are 0.192, 0.256, 0.375, and 0.5. Since the axial position parameter

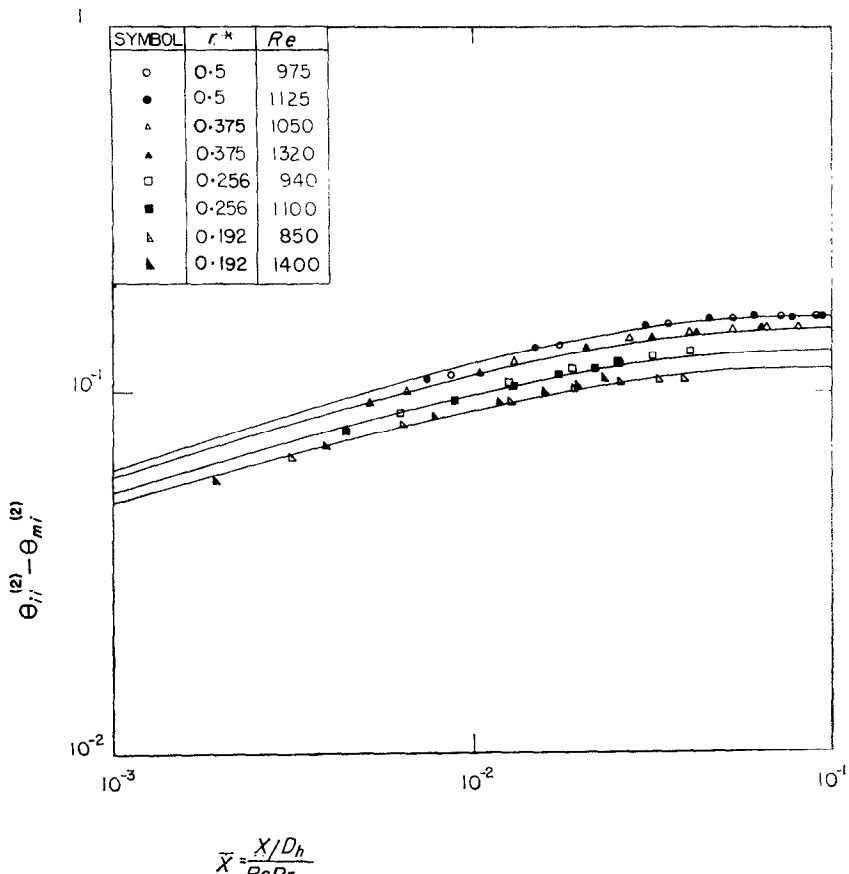


FIG. 14. Comparison of analysis and experiments with the inner wall heated (second kind).

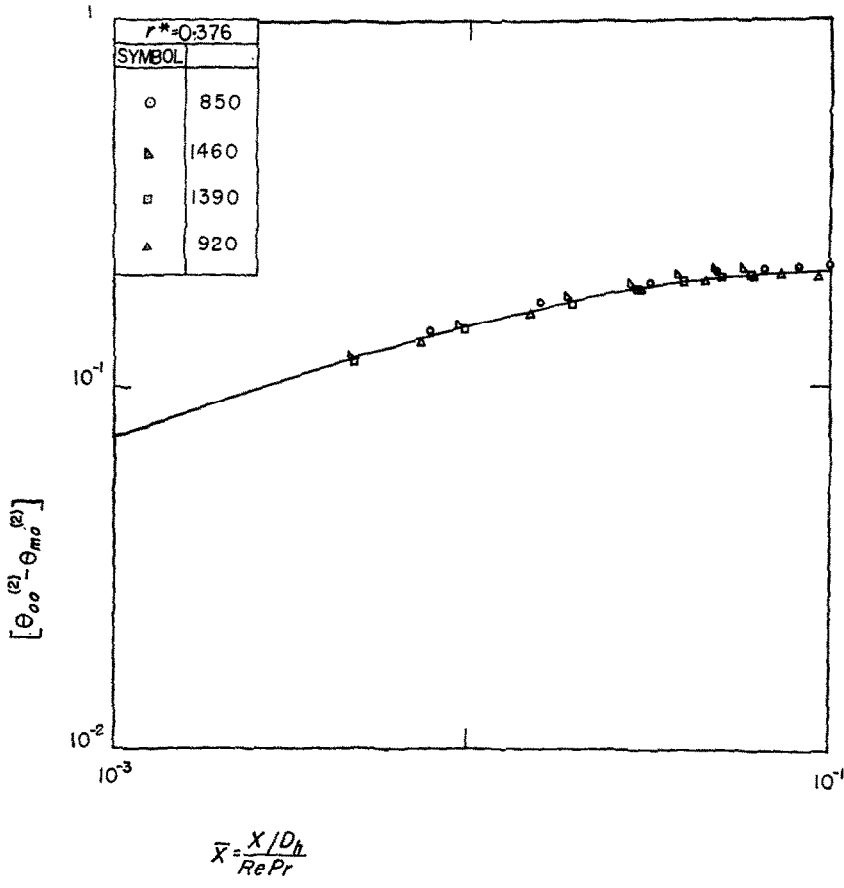


FIG. 15. Comparison of analysis and experiments with the outer wall heated (second kind).

contains the Reynolds number, a range of values of \bar{x} can be generated with fixed axial positions of the thermocouples. Using the method described by Kline and McClintock [15], an uncertainty analysis based on 20 to 1 odds was performed. On this basis, it is felt that the data for heating at the inner wall have a probable uncertainty of ± 5 per cent.

All of the data are within this interval of the theoretical value and most of the points are considerably better. The tendency of the data to lie somewhat low at the first station (small \bar{x}) may be due to an insufficient hydrodynamic entry length or to axial conduction in the tube wall.

When the outer wall is heated, the variation of the fundamental solutions with r^* is much less

pronounced. Accordingly, since the heat loss through the insulation in laminar flow was a significant fraction of the heat input, only the smaller outer tube (1.0 in i.d.) was run in this condition.

The results are shown in Fig. 15 for $r^* = 0.376$. The probable uncertainty in this data is ± 7.3 per cent. Again all of the data lie well within this interval. It should be pointed out that the data for the outer wall heated do not really represent a constant heat flux situation; but because of the dependence of the heat leakage on the tube wall temperature, the heat flux declines about 10 per cent over the range of axial stations at which $\theta_{oo}^{(2)} - \theta_{mo}^{(2)}$ was evaluated. The general good agreement of the data with the theory suggests that if the axial heat flux

variation is not too severe the local wall-to-mean temperature difference can be estimated from the constant flux solution without serious error.

EXAMPLES OF SUPERPOSITION OF THE FUNDAMENTAL SOLUTIONS

The fundamental solutions are particularly convenient for rapid calculations involving superposition of the elementary boundary conditions. To illustrate this computation let us consider some specific examples.

1. Heat flux specified on one wall, temperature on the other

Assume that the heat flux on the inner wall is as shown in Fig. 16, while the outer wall is held at 212°F. The fluid is air which enters at 70°F with a Reynolds number of 1428. The outer tube is 4 inches in inside diameter, the core tube 1 inch in outside diameter. The tubes are 150 in long. We seek the temperature at the inner wall, the fluid mean temperature, and the heat flux at the outer wall as functions of axial position. The pertinent physical constants are, $r^* = 0.25$, $D_h = 0.25$ ft, $Re Pr \approx 1000$.

This problem will require the superposition of Cases 3 and 4. Let us approximate the cosine

distribution by the steps shown in Case 16. If ξ_n is the value of \bar{x} at which the step of heat flux, q''_{in} , is applied, we will have the following:

ξ_n	$q''_{in} D_h/k (\text{ft})$
0	10
0.005	100
0.015	90
0.035	90
0.045	100
0.050	10

We can obtain the inner wall temperature from

$$t_i(\bar{x}) = 70 + 142 \theta_{in}^{(3)}(\bar{x}) - \sum (q''_{in} D_h/k) \theta_{in}^{(4)}(\bar{x} - \xi_n). \quad (48)$$

The summation is taken only of those steps for which $\bar{x} > \xi_n$. Similarly, the outer wall heat flux is given by

$$q''_{out}(\bar{x}) = \frac{k}{D_h} \left[142 \Phi_{in}^{(3)}(\bar{x}) - \sum \left(q''_{in} \frac{D_h}{k} \right) \Phi_{in}^{(4)}(\bar{x} - \xi_n) \right] \quad (49)$$

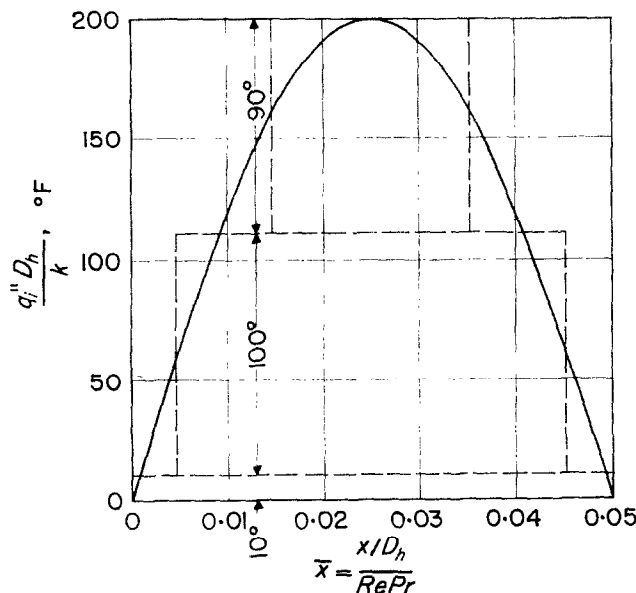


FIG. 16. Cosine heat flux example.

and the mean temperature by

$$t_m(\bar{x}) = 70 + 142 \theta_{mo}^{(3)}(\bar{x}) + \sum \left(q_{in} \frac{D_h}{k} \right) \theta_{mi}^{(4)}(\bar{x} - \xi_n). \quad (50)$$

These values are shown in Figs. 17 and 18. As an example of the calculation consider the axial station $\bar{x} = 0.01$:

$$t_i = 70 + (142)(0) + (10)(0.106) + (100)(0.0868)$$

$$t_i = 79.7^\circ\text{F}$$

$$q_o'' = (0.0146/0.25) [(142)(4.28) - (10)(0.0004) - (100)(0)]$$

$$q_o'' = 609 \text{ Btu/h ft}^2$$

$$t_m = 70 + (142)(0.225) + (10)(0.008)(100)(0.004)$$

$$t_m = 102.4^\circ\text{F}.$$

Notice that in this example, even though heating is taking place at the inner wall, the inner wall temperature is below the mean temperature. This is due to the strong influence of the hot outer wall.

2. Heat flux specified on both walls

This is a situation which could be set up experimentally. The inner wall heat flux is essentially constant at an arbitrary level but the flux at the outer wall decreases with \bar{x} since the heat loss through the insulation increases with the wall temperature.

The radius ratio is 0.376. The values of the fundamental solutions were taken from cross plots made up from Tables 13 and 14.

The results of an asymmetrically heated run are shown in Figs. 19 and 20. The wall heat fluxes were approximately equal. The actual

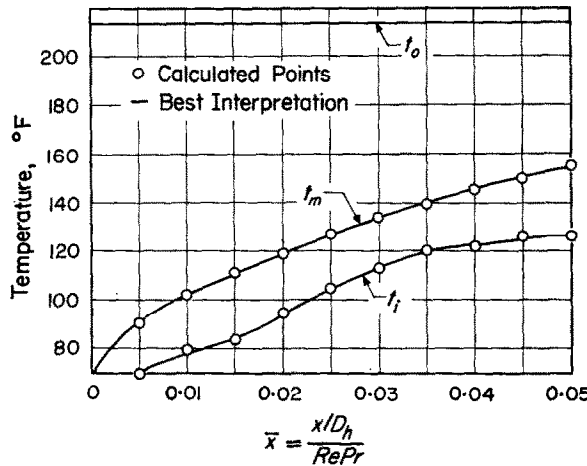


FIG. 17. Temperatures for first example.

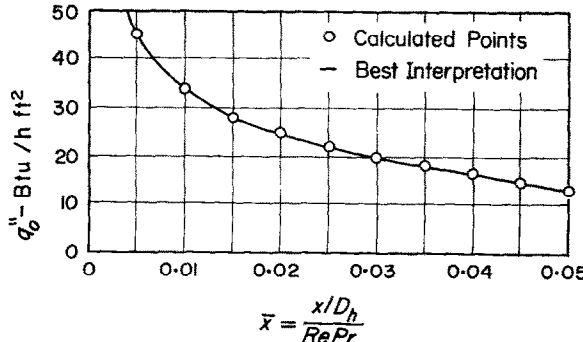


FIG. 18. Outer wall heat flux for first example.

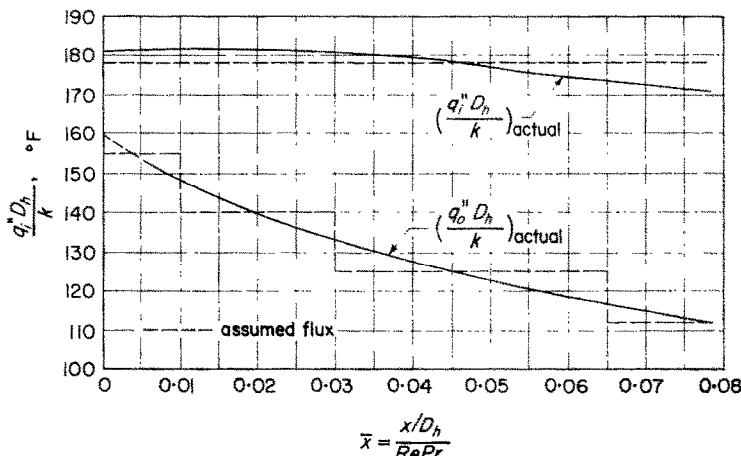


FIG. 19. Heat fluxes for second example.

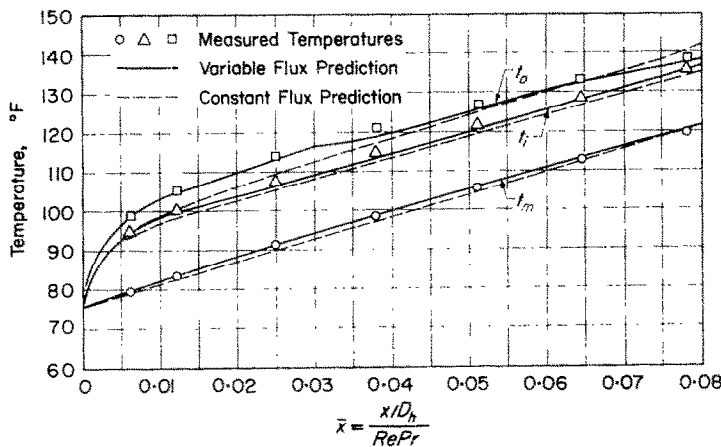


FIG. 20. Comparison of predicted and measured surface temperatures in second example.

wall fluxes as they were measured (corrected for radiation interchange and heat leak) are shown in Fig. 19 together with the approximate distributions chosen to represent them. A comparison of the actual and predicted temperatures is shown in Fig. 20.

The fluid mean temperature is computed from

$$t_m(\bar{x}) = 75.7 + 178 \theta_{mi}^{(2)}(\bar{x}) - \sum_n (q_o'' D_h/k)_n \theta_{mo}^{(2)}(\bar{x} - \xi_n) \quad (51)$$

where ξ_n is the value of \bar{x} for which the n th step of heat flux is applied. Similarly

$$\begin{aligned} t_o(\bar{x}) &= t_m(\bar{x}) + 178 [\theta_{oi}^{(2)}(\bar{x}) - \theta_{mi}^{(2)}(\bar{x})] \\ &\quad - \sum_n (q_o'' D_h/k)_n [\theta_{oo}^{(2)}(\bar{x} - \xi_n) - \theta_{mo}^{(2)}(\bar{x} - \xi_n)] \end{aligned} \quad (52)$$

and

$$\begin{aligned} t_o(\bar{x}) &= t_m(\bar{x}) + \sum_n (q_o'' D_h/k)_n [\theta_{oi}^{(2)}(\bar{x} - \xi_n) \\ &\quad - \theta_{mo}^{(2)}(\bar{x} - \xi_n)] + 178 [\theta_{oi}^{(2)}(\bar{x}) - \theta_{mi}^{(2)}(\bar{x})]. \end{aligned} \quad (53)$$

The summations include only those steps for which $\bar{x} > \xi_n$.

As a comparison the wall temperatures were

computed assuming the wall fluxes were both constant at their average values. This prediction is shown as the dashed line in Fig. 20. While this prediction represents the wall temperatures less well than the multi-step approximation, it is still reasonable since the actual axial variation of the heat flux is not severe. Notice that the constant flux prediction deviates from the measured values most on the outer wall, near the step, where the actual wall flux is varying most rapidly.

REFERENCES

1. W. C. REYNOLDS, R. E. LUNDBERG and P. A. MCCUEN, Heat transfer in annular passages—General formulation of the problem for arbitrarily prescribed wall temperatures or heat fluxes, *Int. J. Heat Mass Transfer*, **6**, 483 (1963).
2. L. GRAETZ, Über die Wärmeleitfähigkeits von Flüssigkeiten, *Ann. Phys. Chem.* **18**, 79 (1883).
3. J. R. SELLARS, M. TRIBUS and J. S. KLEIN, Heat transfer to laminar flow in a round tube or flat conduit—The Graetz problem extended, *Trans. ASME*, **78**, 441 (1956).
4. R. SIEGEL, E. M. SPARROW and T. M. HALLMAN, Steady laminar heat transfer in a circular tube with prescribed wall heat flux, *Appl. Sci. Res. A* **7**, 386 (1958).
5. P. A. MCCUEN, Heat transfer with laminar and turbulent flow between parallel planes with constant and variable wall temperature and heat flux. Ph.D. Dissertation, Stanford University (1961).
6. M. JAKOB and K. A. REES, Heat transfer to a fluid in laminar flow through an annular space, *Trans. AIChE*, **37**, 619 (1941).
7. K. MURAKAWA, Heat transmission in laminar flow through pipes with annular space, *Trans. Jap. Soc. Mech. Engrs.*, **88**, 19, 15 (1953).
8. K. MURAKAWA, Analysis of temperature distribution of nonisothermal laminar flow of pipes with annular space, *Trans. Jap. Soc. Mech. Engrs.*, **18**, 67, 43 (1952).
9. R. VISKANTA, Heat transfer with laminar flow in concentric annuli with constant and arbitrary variable axial wall temperature. Argonne National Laboratories, Report 6441 (1961).
10. R. E. LUNDBERG, W. C. REYNOLDS and W. M. KAYS, Heat transfer with laminar flow in concentric annuli with constant and variable wall temperature and heat flux. Thermosciences Division, Dept. Mech. Engrg. Report AHT-2, Stanford University (1961).
11. M. A. LEVEQUE, Les lois de la transmission de chaleur par convection, *Ann. Min., Paris*, **13**, 201 (1928).
12. V. J. BERRY and C. R. DE PRIMA, An iterative method for the solution of eigenvalue problems, *J. Appl. Phys.* **23**, 195 (1952).
13. R. W. HAMMING, Stable predictor-corrector methods for ordinary differential equations, *J. Assoc. Comp. Mach.* **6**, 1, 37 (1959).
14. R. P. LIPKIS, Discussion on reference [3], *Trans. ASME*, **78**, 441 (1956).
15. S. J. KLINE and E. A. MCCLINTOCK, The description of uncertainties in single sample experiments, *Mech. Engng.*, **75**, 1, 3 (1953).
16. A. P. HATTON and A. QUARMBY, Heat transfer in the thermal entry length with laminar flow in an annulus, *Int. J. Heat Mass Transfer*, **5**, 973 (1962).

Résumé—On présente ici une étude complète du problème thermique dans un écoulement en régime permanent. Elle comprend l'évaluation de quatre solutions fondamentales dans les régions d'énergie thermique par les solutions du problème de valeurs propres comprenant le développement des expressions asymptotiques pour les valeurs propres les plus élevées. Les résultats analytiques sont bien vérifiés par leur excellent accord avec les mesures expérimentales soignées rapportées ici.

Cet article est le second d'une série qui termine quatre années d'études sur les échanges thermiques dans les conduites annulaires.

Zusammenfassung—Es wird eine vollständige Analyse des thermischen Problems in hydrodynamisch ausgebildeter Strömung gegeben. Dies umfasst die Auswertung der vier Grundlösungen in den thermischen Energieräumen durch Lösung des Eigenwertproblems einschliesslich der Entwicklung asymptotischer Ausdrücke für höhere Eigenwerte. Die analytischen Betrachtungen werden durch ihre ausgezeichnete Übereinstimmung mit den hier beschriebenen sorgfältig durchgeföhrten Versuchen bestätigt. Die Arbeit ist die zweite einer Reihe [1], die über eine vierjährige Forschungstätigkeit über Wärmeübergang in Ringräumen berichtet.

Аннотация—Дается развернутый анализ тепловой задачи о гидродинамически полностью развитом течении, включающий в себя вычисление четырех фундаментальных решений для тепловой энергии путем решения задачи о собственных значениях. Разработаны асимптотические выражения для собственных значений большего порядка. Расчетные данные хорошо согласуются с результатами тщательных экспериментальных измерений, приведенными в статье. Данная работа является второй из серии [1] и завершает четырехлетнее исследование теплообмена в кольцевых каналах.